Carbon Capture for Biomass Combustion

Using Precipitating AMP/DMSO System

by Anders Amundsson

LUND
UNIVERSITY

Thesis for the degree of Master of Science
Thesis advisors: Marcus Thern

To be presented, with the permission of the Faculty of Engineering of Lund University, for public criticism on the online meeting at the Department of Energy Sciences on Thursday, the 11th of June 2023 at 09:00.

This degree project for the degree of Master of Science in Engineering has been conducted at the Division of Thermal Power Engineering, Department of Energy Sciences, Faculty of Engineering, Lund University.

Supervisor at the Division of Thermal Power Engineering was Marcus Thern. Supervisor at Kraftringen was Holger Feurstein.

Examiner at Lund University was professor Jens Klingmann.

The project was carried out in cooperation with the Örtofta CHP plant at Kraftringen Energy AB.

Department of Energy Sciences
Faculty of Engineering
Lund University

ISSN: <0282-1990>
LUTMDN/TMHP-23/5547-SE

Typeset in LaTeX
Lund 2023

Contents

List of Figures

List of Tables

Nomenclature

Roman Letters

A	Area	$[m^2]$
A_h	Heat Transfer Area	$[m^2]$
a_i	Specific mass transfer area	$[m^2/m^3]$
$C_{p,i}$	Specific heat capacity at constant pressure of substance i	$[J/kgK]$
F	Mass Flow Rate	$[kg/s]$
FX_y	Mass Flow Rate in stream X of substance y	$[kg/s]$
k	Overall Heat Transfer Coefficient	$[W/m^2K]$
K_G	Overall Mass Transfer Coefficient	$[mole/m^2s]$
M_A	Molar mass of substance A	$[Pa]$
N	Molar flowrate per unit area	$[mole/m^2s]$
N_z^p	Molar flowrate of phase p at position z	$[mole/m^2s]$
N_A^i	Molar flux of component A from the gas phase to liquid phase	$[mole/m^2s]$
p	Purchase cost of equipment	[€]
P_i	Partial pressure of substance i	$[Pa]$
$P_{sat,i}$	Saturation pressure of substance i	$[Pa]$
P_T	Total pressure	$[Pa]$
T	Temperature	$[^\circ C]$
v	Velocity	$[m/s]$

V	Volumetric flow rate [1]	$[Nm^3/\text{h}]$
v_T	Particle settling velocity	$[m/s]$
V_m	Molar volume of ideal gas	$[m^3/\text{mole}]$
x	Molar fraction in liquid phase	$[-]$
x_i	Molar fraction of substance i in liquid phase	$[-]$
y	Molar fraction in gaseous phase	$[-]$
y_i	Molar fraction of substance i in gaseous phase	$[-]$

Greek Letters

ρ	Density of solution	$[kg/m^3]$
ρ_f	Density of fluid	$[kg/m^3]$
ρ_f	Density of particle	$[kg/m^3]$
μ_i	Dynamic viscosity of fluid i	$[mPa/s]$
ΔH	Enthalpy	$[J]$
ΔT_i	Temperature difference of substance i	$[K]$
ΔT_{log}	Logarithmic mean temperature difference	$[K]$
α_{lean}	Loading of CO_2 in solvent in CO_2-lean stream	$[mole/mole]$
α_{rich}	Loading of CO_2 in solvent in CO_2-rich stream	$[mole/mole\ ]$

Abbreviations

BECCS Bio energy carbon capture and storage

CCS Carbon capture and storage

AMP Amino-methyl-propanol

[1] N: "Normal conditions" is subjective and depends on the investigator's preference. Generally, it refers to ambient pressure and "room temperature." It is preferable to specify the actual values or range of temperature and pressure used in the study to accurately describe the experimental conditions.

CAPEX Capital Expenditure

CHP Combined heat and power plant

HPC Hot pottasium carbonate

LMPD Logarithmic mean pressure difference

LMTD Logarithmic mean temperature difference

MEA Mono-Ethanol Amine

DH District heat

Populärvetenskaplig Sammanfattning

Med ökande koncentrationer av koldixodid i atmosfären är den globala uppvärmningen, samt klimatförändringarna ett kritiskt samhällsproblem. För att minska mängden utsläpp av koldioxid har koldioxidavskiljning presenterats som ett alternativ. Koldioxidavskiljning sker genom att rena avgaser från koldioxid för att sedan lagra det i jordskorpan, eller använda i kemiska processer. När tekniken appliceras på en anläggning som förbränner bio-bränslen uppstår potential för netto-negativa utsläpp. Detta eftersom koldioxiden som producerats från förbränningen kommer från träd som har lagrat koldioxid från atmosfären under sin tillväxt, och inte från fossila källor. På Örtofta kraftvärmeverk i södra Sverige ansvänds trä som bränsle för att producera fjärrvärme och el till Eslövs och Lunds kommun.

I det här examensarbete undersöktes möjligheten till koldioxidinfångning på Kraftringens kraftvärmeverk i Örtofta via ett nytt system. Målet var att bedöma lämpligheten för detta system. Systemet som undersöktes var den nya tekniken AMP (2-amino-2-metyl-1-propanol) i DMSO (dimetylsulfoxid) som studeras på Institutionen för kemiteknik på LTH. Tre huvudfaktorer har undersökts för att bedöma systemets lämplighet: energibehov, platsbehov och investeringskostnad. Energibehovet beräknades genom att använda mass- och energibalanser. Utrustningen designades med hjälp av modeller och generella uppskattningar. Kostnadsuppskattningen baserades på korrelationer och litteraturdata. Resultaten jämfördes med en konventionell koldioxidavskiljningsteknik för att uppskatta systemets lämplighet.

Resultaten visar att energibehovet för AMP i DMSO-systemet är stort. Majoriteten av energibehovet kan däremot integreras med fjärrvärmeströmmarna till och från kraftvärmeverket vilket leder till mycket stora besparingar. En sådan integrering är inte möjlig med konventionella system för koldioxidavskiljning. Platsbehovet är större än en konventionell anläggning, eftersom det undersökta systemet innefattar en extra processenhet. Detta innebär även högre investeringskostnader för anläggningen.

En fullständig lämplighetsbedömning kan inte göras, men AMP i DMSO visar lovande resultat i undersökningen på grund av systemets integreringsmöjligheter. Då det undersökta systemet är relativt nytt är det en del data som har behövts approximeras. Mer forskning behövs för att en mer detaljerad design, samt tekno-ekonomisk analys ska kunna utföras. Kraftringen bör även undersöka vilka effekter energiintegreringen kan medföra för Örtofta kraftvärmeverk.

Abstract

In order to limit global warming, bioenergy carbon capture and storage (BECCS) technologies are getting increased attention. To meet emission scenarios, an estimated 4000 carbon capture plants are expected to be required by 2030, indicating that progress in carbon capture and storage (CCS) deployment is currently lagging behind expectation. Therefore novel technologies for carbon capture and storage are needed.

In this work, the suitability of a novel system for carbon capture, researched at the Department of Chemical Engineering at Lund University, is assessed at a combined heat and power (CHP) plant at Örtofta in the south of Sweden. Three main factors are investigated in order to determine suitability, which include energy demand, equipment design and cost estimation. Energy demand was calculated using energy and mass balances. Equipment design was made using models and rules of thumb. Cost estimation was estimated using correlations and literature data. Results are compared with a conventional system for carbon capture.

The results show that the energy demand of the AMP/DMSO system is large. However, a majority of the heating and cooling to the system could be supplied by the district heat (DH) stream and returning stream. The system require more space than a conventional system due to the addition of a phase separation unit. This also increases the investment cost of the plant.

More research is required to delve into more comprehensive process designs, explore effective CO_2 capture management strategies, and conduct thorough assessments of economic feasibility. Furthermore, the effects on the plant from integrating the CCS plant with the DH cycle needs to be determined. This thesis serves as a valuable guide for future endeavors, providing valuable insights into the design of a carbon capture plant.

Chapter 1.

Introduction

In order to limit global warming and comply with the Paris Agreements, it is essential to significantly reduce anthropogenic carbon dioxide (CO_2) emissions. This will require emission-intensive industries such as steel, cement, and oil refineries to implement carbon capture and storage (CCS) technologies in order to achieve substantial emissions reductions. Integrated assessment models constrained to 2 °C warming show that CCS is necessary for reaching emission targets [1]. However, CCS is associated with high energy requirements and investment costs, making large-scale and cross-sector deployment challenging [2]. To meet emission scenarios, an estimated 4000 CCS plants are expected to be required by 2030, indicating that progress in CCS deployment is currently lagging behind expectations [3].

BECCS (Bio energy carbon capture and storage) is a promising technology that combines biomass utilization with CCS to reduce greenhouse gas emissions and mitigate climate change [4], [5]. In BECCS, biomass, such as plant residues or dedicated energy crops, used as a feedstock for bioenergy production through processes such as combustion or gasification. The resulting bioenergy can be used for electricity generation, heat production, or as a fuel in various industries. The CO_2 released during the bioenergy production process is captured, transported, and stored in underground geological formations, preventing its release into the atmosphere where it would contribute to global warming [4].

1.1. Purpose and Objectives

This thesis was conducted at the Department of Energy Sciences at LTH, Lund University, in collaboration with Kraftringen Energi AB, with the objective of evaluating a novel carbon capture technology for its application at the Örtofta combined heat and power (CHP) plant in south Sweden. The technology assessed a novel technology that has been researched at the Department of Chemical Engineering at LTH. Simplified process design was employed to capture CO_2 from the flue gas streams of the Örtofta CHP plant, and the energy requirements for heating and cooling was estimated, along with the

potential CO_2 capture capacity. Furthermore, equipment dimensions and the investment cost of the proposed CCS plant was estimated.

The objectives of this thesis are as follows:

- To determine the potential amount of CO_2 that could be captured from the Örtofta CHP plant.
- To compare and evaluate the carbon capture technology with others in terms of their energy requirements and suitability for the power plant.
- To identify types and sizes of process units needed for the CCS plant in order to give an estimate on the investment cost of the plant.

The first research question in this thesis is how does the AMP/DMSO system for carbon capture compare to other technologies in terms of energy requirements at the Örtofta CHP plant.

Additionally, the second one is to identify required types and sizes of primary process units for the proposed carbon capture and storage (CCS) plant at the Örtofta CHP plant, and what the estimated investment cost of implementing this CCS plant will be.

1.2. Constraints & Limitations

All estimations are made considering data provided by Kraftringen. The proposed design of the CCS plant is made on boundries surrounding the CCS facility. The process design only focus on the CO_2 separation steps of the plant and does not include specifications on how the captured CO_2 is pressurized and liquified, transported and managed or stored.

Chapter 2.

Background

BECCS is a promising technology that combines biomass utilization with carbon capture and storage (CCS) to reduce greenhouse gas emissions and mitigate climate change [4], [5]. In BECCS, biomass, such as plant residues or dedicated energy crops, is used as a feedstock for bioenergy production through processes such as combustion or gasification. The resulting bioenergy can be used for electricity generation, heat production, or as a fuel in various industries. The carbon dioxide (CO_2) released during the bioenergy production process is captured, transported, and stored in underground geological formations, preventing its release into the atmosphere where it would contribute to global warming [4].

The process of BECCS can be summarized into three main steps: biomass production and collection, bioenergy production, and carbon capture and storage. First, biomass is sustainably produced and collected, either from existing agricultural residues or from dedicated energy crops. Next, the biomass is converted into bioenergy through processes such as combustion, gasification, or anaerobic digestion. During the bioenergy production process, CO_2 is released as a byproduct, which is then captured using various capture technologies such as absorption, adsorption, or membrane separation. The captured CO_2 is then transported to suitable geological formations, such as deep saline aquifers or depleted oil and gas reservoirs, for permanent storage through injection and storage techniques. The stored CO_2 is monitored and verified to ensure its long-term containment and prevent leakage into the atmosphere [4].

BECCS has the potential to achieve negative emissions, as the biomass used in the process absorbs CO_2 from the atmosphere during its growth, and the captured CO_2 is stored underground, effectively removing carbon dioxide from the atmosphere. BECCS has been identified as a key technology in many climate change mitigation scenarios and is considered as one of the most effective ways to achieve large-scale negative emissions to meet climate targets and limit global warming to below 2 °C [4], [5].

2.1. Örtofta Power Plant

The Örtofta Power Plant is a biomass-fired combined heat and power (CHP) plant located in southern Sweden, owned and operated by Kraftringen Energy AB [6]. It plays a significant role in Sweden's transition towards renewable energy and sustainable biomass utilization.

The plant utilizes a CHP system, where biomass, such as wood chips, bark, and agricultural residues, is combusted in a boiler to produce high-pressure steam that drives a steam turbine for electricity generation. The waste heat from the combustion process is captured and used for district heating or other industrial processes, maximizing the plant's energy efficiency [7].

The Örtofta Power Plant has a total installed capacity of 120 MW and produces up to 600 GWh of heat and 200 GWh of electricity annually. [6], [8]. It contributes to Sweden's renewable energy targets and greenhouse gas emissions reduction goals by utilizing sustainable biomass as a renewable and carbon-neutral energy source.

2.2. Carbon Capture at Örtofta Power Plant

Kraftringen Energy AB is expanding the Örtofta Power Plant in southern Sweden to increase its capacity and improve efficiency. The project will involve the installation of a new turbine, which will increase the plant's capacity by 50 %.

Furthermore, the Örtofta Power Plant expansion is designed to be "carbon capture ready," which means that the plant will be able to capture carbon dioxide emissions for storage or use in other industrial processes. The implementation of carbon capture technology is an important step towards reducing greenhouse gas emissions and combating climate change.

According to Kraftringen Energy AB, the expansion of the Örtofta Power Plant is part of their broader efforts to transition to a more sustainable energy mix [9]. The company aims to invest in renewable energy sources and develop carbon capture technology to reduce their carbon footprint and contribute to a more sustainable future.

2.3. Carbon Capture

Carbon capture, also known as carbon capture and storage (CCS), refers to a process in which CO_2 emissions generated by various industrial processes are captured and then stored in underground geological formations. The aim of this process is to reduce

the amount of greenhouse gases, such as CO_2, in the atmosphere, which are a major contributor to climate change.

The process of carbon capture typically involves three main steps: capture, transport, and storage. The capture phase involves the collection of CO_2 from industrial sources, such as power plants, refineries, and cement factories, before it is released into the atmosphere [10]. Once the CO_2 has been captured, it must be transported to a storage site. This is typically done through pipelines or ships [11]. Finally, the CO_2 is stored underground in geological formations, such as depleted oil and gas reservoirs, deep saline formations, or unmineable coal seams.

Various techniques can be employed for carbon capture, including physical and chemical absorption, adsorption, and membrane separation. This thesis focus on absorption. In absorption, a liquid absorbent in a solution with a solvent is utilized to separate CO_2 from the gas stream by dissolving and potentially reacting with it. The CO_2-rich phase is then transported to another container where conditions are altered, allowing for the release, capture, and potential storage of CO_2.

Commonly used absorbents for CO_2 capture are alkanolamines and carbonates. Alkanolamines are often referred to as amines in literature related to carbon capture, and this thesis will also use the term ”amines”. Amines are selective to acid gases such as CO2 and H2S and have been employed since the 1930s, originally for removing CO2 from natural gas or hydrogen. Monoethanolamine (MEA) is an example of an extensively studied and commercially used amine. Other examples include methyldiethanolamine (MDEA) and the sterically hindered aminomethylpropanol (AMP). Carbonates, such as potassium and sodium carbonates, are also used for carbon capture. The traditional Benfield process, which employs hot potassium carbonate (HPC), has been utilized since the 1950s for removing CO2 and H2S from synthesis gas and represents another commercially viable carbon capture technology [10]. This work will only investigate amine absorption systems.

2.3.1. The MEA Process

The MEA process is widely considered to be the base case of carbon capture process [11]–[13]. Therefore, it will be used in comparison to results made in this work. A simplified process flowchart of the MEA process is seen in Figure 2.1. Water is condensated from the flue gas in order to increase the CO_2 concentration. It then enters an absorption column where the gas is absorbed in to a liquid solvent through a series of chemical reactions. The dissolved CO_2 and the solvent is then fed to a desorption column, commonly a stripping column, where conditions are altered using heat. CO_2 is evaporated from the solvent and is reclaimed and fed to a liquefaction process [13]. The liquid solvent is recirculated to the absorption column. In Figure 2.1, streams with a high concentration of CO_2 (CO_2-rich) are marked red, while streams with low concentration of CO_2 (CO_2-lean) are marked blue. It is common to utilize the heated liquid stream

from the stripping column in order to pre-heat the stream containing dissolved CO_2 [11]. The unit where this is done is called the Rich-lean Heat Exchanger.

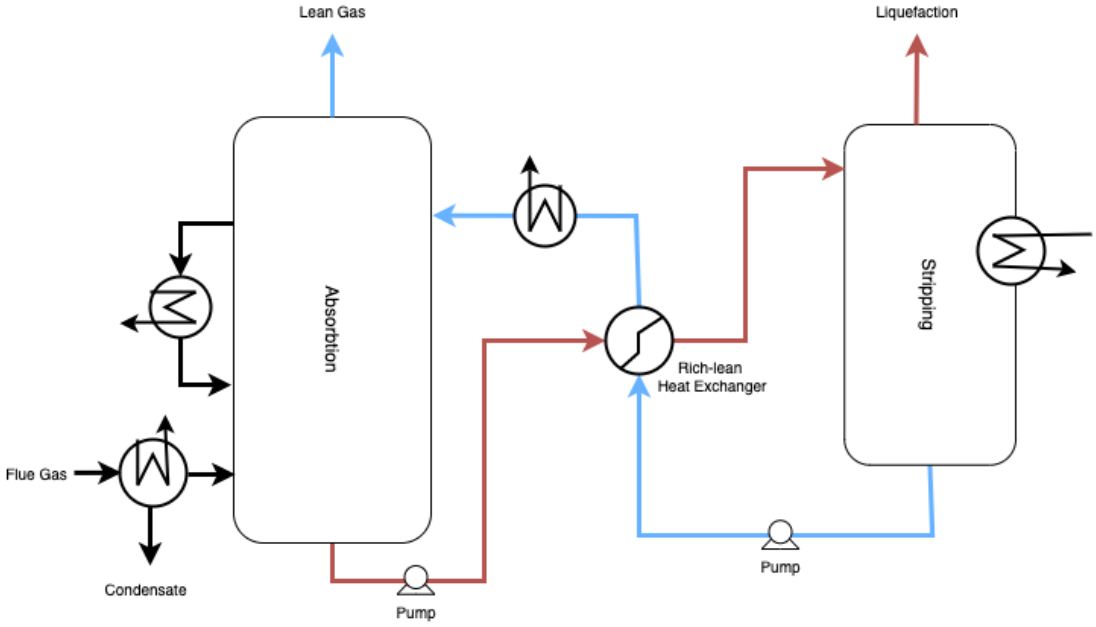

Figure 2.1.: Simplified process flowsheet of a conventional amine absorption system for carbon capture.

2.4. Carbon Capture Using Precipitating Amine Systems

Carbon capture using precipitation of amine and organic solvents is a system that has been studied by researchers at Lund University, including Hanna Karlsson and Helena Svensson [14]–[16]. The amine used in these systems is 2-amino-2-methyl-1-propanol (AMP), which is a sterically hindered primary alkoanol amine [14]. The chemical structure of AMP can be viewed in Figure 2.2.

When carbon dioxide (CO_2) is absorbed into AMP, both physical absorption and a reaction between AMP and CO_2, resulting in AMP carbamate formation, enhance the absorption [13]. The theoretical maximal loading of CO_2 in AMP is 0.5, but a higher loading could be achieved if the solvent also participates in the reaction. If the solvent does not participate in the reaction, the sterically hindered AMP induces solid precipitation of the carbamate salt [13]. This precipitation enables the use of a phase separator to separate the liquid solvent from the solid precipitate of AMP/CO_2, making it possible to recirculate the solvent to the absorber, and leaving less of the mixture to be heated in the regenerator.

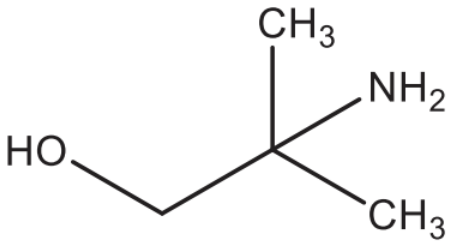

Figure 2.2.: Chemical structure of AMP.

One system that has been studied extensively is the AMP/NMP system [12], [13]. The solubility of CO_2 in AMP/NMP has been evaluated for various compositions and temperatures. Precipitation was observed in the temperature range of 25 - 40 °C for 15 wt% AMP/NMP (15A - N) and 25-50 °C for 25 wt% AMP/NMP (25A - N). The rate of absorption (flux) was determined using a wetted wall column (WWC) and was found to increase linearly with logarithmic mean pressure difference (LMPD) [17]. However, it is worth noting that NMP is a reproductively toxic substance [18], which may limit its practical applicability in large-scale carbon capture processes.

In light of the potential toxicity concerns associated with NMP, researchers have investigated other solvents in combination with AMP for precipitation-based carbon capture systems. Further studies have been conducted to evaluate the solubility of CO_2 and precipitating properties of AMP with a variety of solvents, with the aim of identifying alternative solvents that are environmentally benign and commercially viable. Seven organic solvents were investigated in mixtures with 25 wt% AMP namely, di-methyl-sulph-oxide (DMSO), 1-pentanol (1P), 3-(dimethylamino)propionitrile (DMAPN), propylene carbonate, 4-heptanone, 1-methyl imidazole and cyclohexanol, at low temperatures (25-40 °C) [13]. From recent research it was suggested that the system of AMP in DMSO was the most promising solvent and was therefore investigated further [16].

2.5. AMP in DMSO

A new non-aqueous absorption system based on AMP dissolved in DMSO has been identified as a promising candidate for capturing CO_2. Compared to the conventional NMP-based system, the AMP/DMSO system exhibited higher CO_2 solubility at all tested temperatures, while maintaining similar precipitation characteristics [13]. Although the CO_2 solubility of the non-aqueous systems were lower than that of the benchmark MEA solution, the cyclic capacities could still be comparable under suitable absorption conditions. The cyclic capacity is the value of difference of CO_2 loading at absorption and regeneration conditions [15]. It is used to compare CCS technologies.

$$\alpha_c = \alpha_{rich} - \alpha_lean \tag{2.1}$$

The advantages of the novel systems include the use of low-grade heat for regeneration, without requiring a stripping agent at atmospheric pressure.

The experiments also revealed that increasing the amine concentration enhances the CO_2 solubility and enables precipitation at higher temperatures and lower CO_2 loadings [16]. However, the heat of absorption tends to increase with the onset of precipitation, which could lead to hot spots within the absorption column. Since the organic solvents have lower heat capacities than water, intercooling may be necessary to ensure precipitation occurs along the entire column.

The presence of water in the DMSO solvent could cause water accumulation and affect the absorption capacity. However, water accumulation up to a certain molar ratio did not affect precipitation or regeneration efficiency. The presence of water may also limit the temperature rise in the column due to its high heat capacity and greater volatility [13]. It may also facilitate bicarbonate formation, allowing for higher CO_2 loadings. Nonetheless, water could also lead to quicker amine degradation, as indicated by 13C NMR studies [16].

The absorption of CO_2 into AMP involves both physical absorption, as depicted in Reaction 2.2, as well as a chemical absorption through reaction between AMP and CO_2. This reaction leads to the formation of AMP-carbamate, which further enhance the absorption, as described in Reaction 2.3.

$$CO_2(g) \rightleftharpoons CO_2(sol) \tag{2.2}$$

$$CO_2(sol) + 2RNH_2(sol) \rightleftharpoons RNH_3^+(sol) + RNHCOO^- \tag{2.3}$$

If the solvent does not participate in the reaction, the steric hinderence of AMP induces the precipitation of solid carbamate salt [13].

$$RNH_3^+(sol) + RNHCOO^-(sol) \rightleftharpoons [RNH_3]^+[RNHCOO]^-(s) \tag{2.4}$$

The physical and chemical interactions due to Reactions 2.2, 2.3 and 2.4 are further illustrated in Figure 2.3.

In light of the promising research conducted at the Department of Chemical Engineering, a collaborative project involving Växjö Energi AB (VEAB), Sydskånes Avfallsaktiebolag (SYSAV), Öresundskraft, and Granitor was launched in 2021, with funding from Energimyndigheten. The primary objective of this project is to construct a pilot plant, facilitated by Granitor, and subsequently operated at VEAB, SYSAV, and Öresundskraft.

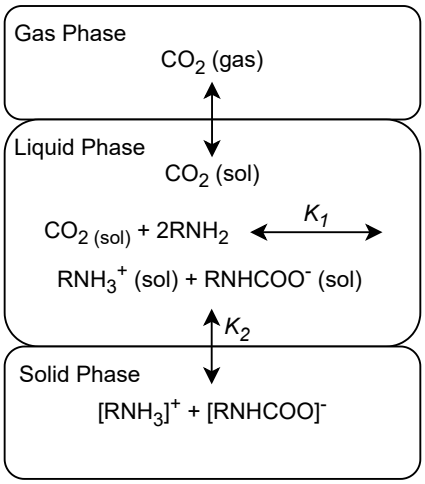

Figure 2.3.: Physical and chemical interactions in the system. Adopted from M. Sanku [12].

The purpose of this pilot plant is to evaluate the practical implementation AMP/DMSO system.

Chapter 3.

Methods

The working process of this thesis can be divided into three different phases, illustrated in Figure 3.1. The heat phase which aims to investigate the heating and cooling demand of the process using mass and energy balances. The equipment phase where the primary and secondary equipment are sized in order to estimate the space requirements. Lastly, the cost phase where the direct capital cost is estimated using literature correlations.

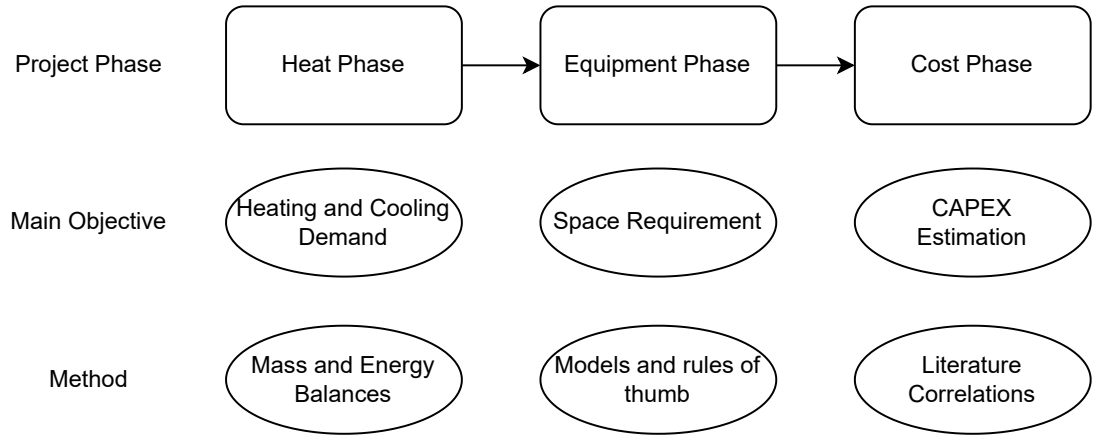

Figure 3.1.: Working process of the project, simplified into three main phases.

Figure 6 illustrates the working methodology of this thesis. The process began with a simple design of the process being created created, and data needed for calculations was collected from various sources. The obtained data was then used to calculate the mass balance of the processes and determine the heating, cooling, and electricity demands in the energy balance. Simultaneously, sources of available excess heat at the plant were identified, and calculations were performed to estimate the amount of available heat from each source. An evaluation of the energy demands and available excess heat was performed to determine if the available excess heat could meet the heat demands of the capture process. Sizing of equipment and unit dimensions are then carried out. A simplified model for the absorption column was developed and simplified methods were used to estimate the rest of the units. The unit dimensions are then used for the

direct capital expenditure estimation. Additionally, a sensitivity analysis was conducted to evaluate the influence of uncertain data on the results. The work was performed iteratively, and more information on the different parts of the working process is presented in the following subsections.

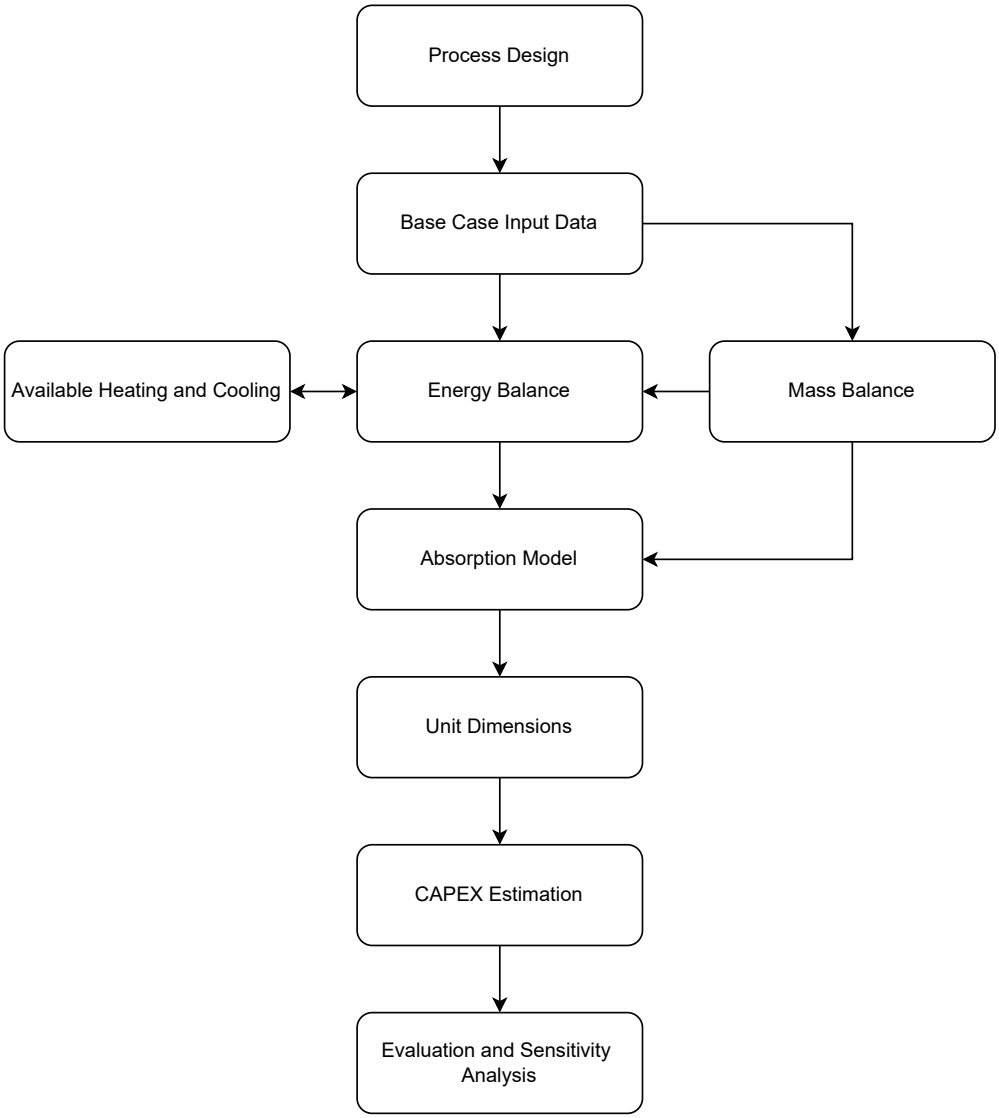

Figure 3.2.: Schematic view of the project methodology.

3.1. Process Design

Because of the precipitation of the carbamate salt in the absorption, the process of a non-aqueous CCS plant differs slightly from the conventional aqueous systems, like in Figure 2.1. A simplified process chart of the AMP/DMSO system is viewed in Figure 3.3.

The main differences between Figures 2.1 and 3.3 is the addition of a phase separation (Phase Sep in Figure 3.3) unit between the absorption and desorption units. The aim of the phase separation is the separation of the liquid solvent DMSO and non-precipitated AMP from the CO_2-rich stream. This has the effect of decreasing the amount of substance that needs to be heated in the desorption unit. As mentioned, the desorption is often the prime contributor to the energy demand of a CO_2 capturing process. Consequently, the amount of substance fed to the unit is likely to have a large impact on the energy demand of the entire process.

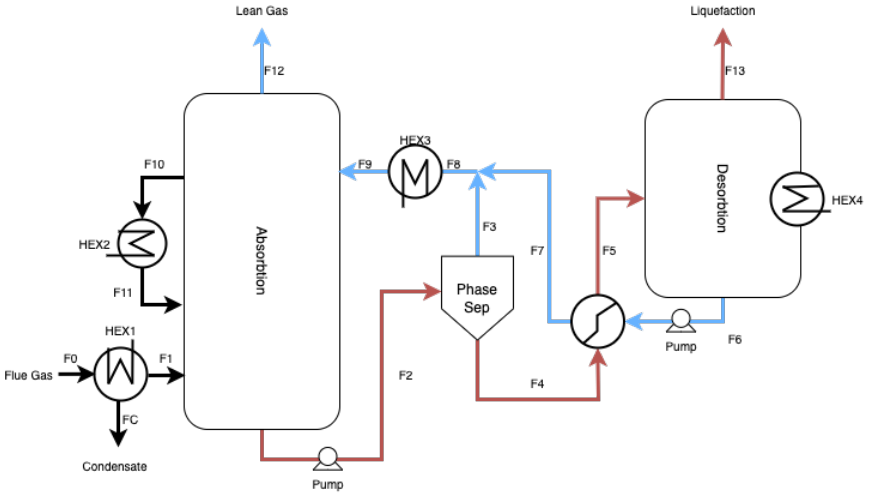

Figure 3.3.: Simplified flow chart of a non-aqueous precipitating CCS process.

3.2. Base Case Input Data

For the base case, data was gathered from a report made by Captimise*[19], who made a report on a planned carbon capture-ready expansion of Örtofta CHP. These values are estimated, and was later replaced by gathered data from Kraftringen's data base. The values used as input includes, volumetric flow of the flue gas, temperature of the flue gas, CO_2 concentration and H_2O concentration. NO_x concentration is also a very significant property, when designing an amine absorption CCS plant. This is due to the formation of toxic N-nitrosamines [20][21]. It was, however, determined that the NO_x levels in the flue gas was too high to manage any amine carbon capture system. There are measures available to reduce the NO_x concentration in the flue gases, and this thesis therefore assumes that these have been installed. The input data is viewed in Table 3.1. All the values are estimated by Captimise.

In order to design the absorption column, parameters regarding the solubility of CO_2 and the heat of absorption is needed from literature. These are summarized in Table 3.2.

Table 3.1.: Base case input data from Captimise report. [19]

Property	**Abbreviation**	**Value**	**Unit**
Flue gas flow flow rate	V_{fg}	190000	Nm^3/h
Temperature	T	45	^oC
CO_2	y_{CO_2}	13	Vol%
H_2O	y_{H_2O}	10	Vol%
Rest (air)	y_{air}	77	Vol%
Capture rate	r_c	90	Mol%

Table 3.2.: Important parameters from the research papers, used in this work.

Property	Value	Source
α_{rich}	0.32	[13]
α_{lean}	0.08	[14]
ΔH_{abs}	56	[15]

3.3. Mass Balance Calculations

The mass balance calculations was made based on the data in Table 3.1. They were, however, generalised so that the input data could be altered when internal data was collected. For simplicity the flue gases are treated as containing three components - CO_2, water and air. The total mass flows of the components can be calculated by treating the flue gas as ideal gas.

$$F0_A = \frac{V_{fg} y_A M_A}{V_m} \tag{3.1}$$

In Equation 3.1, the total volumetric flowrate of the flue gases, V_{fg} is multiplied by the molar fraction of component A, y_A, and the molar mass of component A, M_A. This is further divided by the molar volume of an ideal gas, V_m, in order to get a mass flow of component A expressed in kmole/h.

Because the absorption in the AMP/DMSO is modelled as a water free system, water needs to be separated from the flue gas by a flue gas condenser. In order to estimate how much water that is separated, it is assumed that the flue gas is saturated with water and that the liquid phase only contains pure water.

The partial pressure of the water in the cooled flue gas is described by Raoult's Law.

$$P_{H_2O} = P_{sat,H_2O} x_{H_2O} \tag{3.2}$$

Furthermore the water content in the cooled flue gas can be estimated using Dalton's law

$$P_{H_2O} = y_{H_2O} P_{tot} \tag{3.3}$$

It is assumed that the CCS plant separates 90 % of the CO_2. From this assumption an overall mass balance can be made.

By assuming that no CO_2 is dissolved in the DMSO, the amount of AMP needed for the absorption is calculated from Equation 3.4. The rich and lean loading of the systems are taken from Table 3.2.

$$F9_{AMP} = \frac{F9_{CO_2}}{\alpha_{rich}} \tag{3.4}$$

$$F9_{DMSO} = F9_{AMP} + 3 \cdot F9_{AMP} \tag{3.5}$$

From the above data and the additional assumption of no AMP/DMSO evaporating gas phase, it is possible to calculate CO_2 and solvent mass balances over the absorption unit according to Equations 3.6-3.8.

$$F1_{CO_2} - F2_{CO_2} - F12_{CO_2} + F9_{CO2} = 0 \tag{3.6}$$

$$-F9_{solvent} + F2_{solvent} = 0 \tag{3.7}$$

$$F1 - F2 - F12 + F9 = 0 \tag{3.8}$$

3.4. Energy Balance Calculations

Energy balances over the system and over specific components and heat exchangers were made in order to determine the temperature of the streams, as well as the heating and cooling requirements of the system.

The energy balances are made considering a few general assumptions. The heating and cooling of the streams are made under constant pressure, there are no phase changes, the specific heat capacity (C_p) remains constant and the system is closed to mass and energy losses [22]. Then the heat released or taken up (Q) by a stream that undergoes a temperature change, T_1 to T_2, can be described by the following equation.

$$\dot{Q} = \dot{m} C_p (T_2 - T_1) \tag{3.9}$$

C_p of a fluid that changes in temperature in a heat exchange is approximated as the weighted average C_p of the fluid.

$$C_p(T_1 \rightarrow T_2) = \left(\frac{C_{p,T_1} - C_{p,T_2}}{2} \right) \tag{3.10}$$

If C_p is not available for a fluid, the fluid is treated as ideal and C_p can be estimated by average C_p of each component in the fluid

$$C_{p,avg} = \frac{\sum C_{p,i} \dot{m}_i}{\dot{m}} \tag{3.11}$$

It is assumed that the dissolved CO_2 does not affect the specific heat capacity of the fluid. Instead, the heat capacity is estimated by the amounts of AMP and DMSO in the stream. Using Equation 3.11, there are two different specific heat capacities that are needed. One before the phase separation unit and one after. These will be denoted $C_{p,post}$ and $C_{p,pre}$ for post- and pre-separation respectively.

The amount of heat released when absorbing CO_2 can be estimated by the experimentally measured heat of absorption at 50 °C (ΔH_{abs}) [13].

$$\dot{Q}_{abs} = \Delta H_{abs} \cdot \dot{m}_{CO_2,abs} \tag{3.12}$$

In order to keep the absorption column at constant temperature, internal cooling is needed. The energy required for the internal cooling of the absorption column is assumed to be equal in magnitude to the heat of absorption calculated through Equation 3.12. The energy released during the absorption is assumed to be equally distributed in the liquid and gas phase. Consequently, the streams leaving the absorption column are assumed to have the same temperature.

The phase separation unit is considered to have no energy losses and therefore the streams entering this unit are considered to have the same temperature.

Heat recovery is possible within the process. The absorption is considered to be operated at a temperature of 50 °C and the desorption is operated at 88 °C. The rich stream entering the desorption unit can therefore be pre-heated using excess heat from the lean stream that leaves the desorption unit. In this work, this unit is referred to the rich-lean heat exchanger. The minimum temperature difference (ΔT_{MIN}) in a counter current heat exchanger is located at the inlet of the cold stream and outlet of the hot stream, illustrated in Figure 3.4 [23]. Assuming a counter current heat exchanger and a ΔT_{MIN} of 10 °C, the heat recovery and the temperatures of streams leaving the rich-lean heat exchanger can be estimated.

$$T_{F7} = T_{F4} + \Delta T_{MIN} \tag{3.13}$$

The heat recovery can then be estimated by the following equation.

$$\dot{Q}_{rich-lean} = \dot{m}_h C_{p,post}(T_{des} - T_{F7}) \tag{3.14}$$

where $Q_{rich-lean}$ is the heat recovery within the rich-lean heat exchanger, m_h is the mass of the hot stream and T_{des} is the desorption temperature.

Assuming no heat losses, the energy balance of the rich-lean heat exchanger can be rearranged in order to solve for the outlet temperature of the cold stream.

$$T_{F5} = \frac{\dot{Q}_{rich-lean}}{\dot{m}_c C_{p,post}} + T_{F4} \tag{3.15}$$

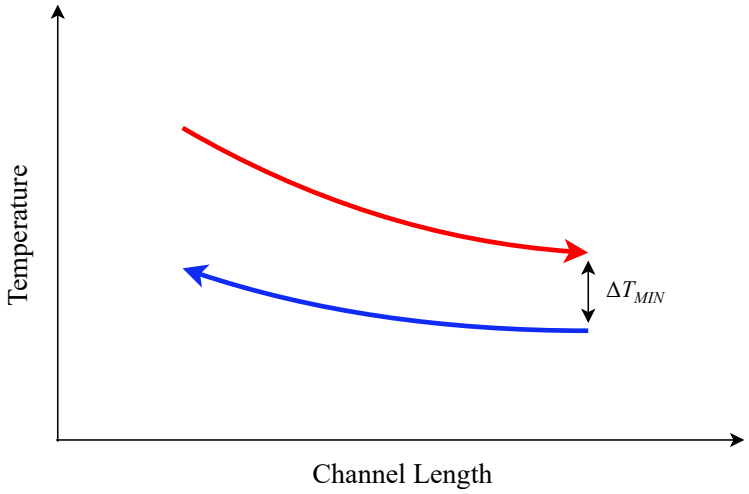

Figure 3.4.: Illustrative figure of the principle of ΔT_{MIN} for a counter current heat exchanger. The minimal temperature difference is located at the outflow of the hot stream and the inflow of the cold stream. Adopted from R. Smith [23].

The desorption unit operates at a temperature of 88 °C, the inflow temperature is calculated using Equation 3.15. The sensible heat, Q_{sens}, or the heat required to raise the temperature of the fluid to the desorption temperature, is calculated by

$$\dot{Q}_{sens} = C_{p,post}\dot{m}_{F5}\Delta T \tag{3.16}$$

Assuming that the same heat released during absorption needs to be taken up in order to

reverse the reaction, heat required for desorption is calculated by

$$\dot{Q}_{des} = \Delta H_{abs} \cdot \dot{m}_{CO_2,des} \tag{3.17}$$

The heat of absorption is lower at 88 °C than at 50 °C. Experiments on the desorption heat is, however, yet to be made. Therefore, lower desorption heat could be very possible. Sensitivity analysis on the ΔH_{abs} is carried out in order to see how much influence a lower value for ΔH_{abs} has on the total energy demand.

3.4.1. Heat integration using district heat outflow and returning flow

The main advantages with the AMP/DMSO system for carbon capture is the ability to desorb at low temperatures while still maintaining a relatively large cyclic capacity [24]. For a conventional MEA process, and most other aqueous systems for carbon capture, desorption is done by a stripping column, known as stripper [13]. The stripper needs low pressure (LP) steam in order to operate, because the desorption temperature is usually above the boiling point of water (>100 °C). Because the steam needs to be generated, this is going to account for a direct loss of power, resulting in less heat or electricity production.

The AMP/DMSO process studied in this work has a desorption temperature of 88 °C, which means that heating medium can be liquid, high temperature water. Örtofta CHP combusts biomass in order to generate electricity and district heat (DH). Temperatures and volumetric flow rates of the DH and the return stream are seen in Table 3.3. The average temperature of the DH is 97 °C while the average temperature of the returning DH is 42 °C. The average volumetric flow rate is approximately 1800 m^3/h.

Table 3.3.: Temperatures of the district heat stream and the return stream. The average temperatures are used in this work. [Internal report from Kraftringen AB]

Property	Unit	DH	Return
T_{Min}	°C	86	53
T_{Max}	°C	105	37
T_{Avg}	°C	97	42
V_{Avg}	m^3/h	1800	1800

The heating and cooling utility available by the DH streams are estimated using the flow rates in Table 3.3 and Equation 3.9.

3.5. Equipment Dimensions

This section covers the methods used in order to estimate the required sizes of the primary equipment needed within the CCS plant. Only primary equipment are being included in the analysis. The primary equipment are the absorption unit, the phase separation unit and the desorption unit. The secondary components are the pumping units and the heat exchanger units.

3.5.1. Absorption Unit

The design of an absorption column involves several key steps to ensure efficient and effective mass transfer between a gas and a liquid phase. In this section, a methodology for designing an absorption column is introduced, encompassing the following aspects: selection of packing and the mass transfer area, selection of liquid velocity, estimation of flooding velocity, determination of the cross-sectional area, calculation of liquid flowrate, and estimation of packing height. Specifications and parameters are presented in Appendix B.

The first step in the design process is the selection of an appropriate packing for the absorption column. The choice of packing depends on various factors such as the nature of the gas and liquid phases, desired mass transfer efficiency, pressure drop limitations, and cost considerations. Commonly used packing materials include structured packings (e.g., metal, plastic), random packings (e.g., Raschig rings, Pall rings), and structured grids [25]. Structured packings are often more expensive than random packings [26]. They are, however, more suitable for larger absorption columns as they ensure an more equal liquid distribution than random packings [25]. The choice of packing is also influenced by the precipitation within the absorption column. If the geometric surface area (a_g) is too high, clogging might be an issue.

The liquid velocity in the absorption column plays a crucial role in achieving efficient mass transfer. It is determined based on the desired level of gas-liquid contact and the specific characteristics of the packing material. The liquid velocity is typically selected to ensure adequate wetting efficiency of the packing surface without causing excessive pressure drop [25].

To achieve the desired level of mass transfer, it is essential to determine the required mass transfer area. The mass transfer area is influenced by factors such as the composition of the gas and liquid phases, desired separation efficiency, and the equilibrium relationship between the phases.

Flooding is a critical phenomenon that occurs when the gas flowrate becomes too high, leading to a loss of interfacial area and reduced mass transfer efficiency [25]. To prevent flooding, the maximum gas velocity or flooding velocity needs to be estimated. Empirical correlations, based on the characteristics of the packing and the fluid properties, can be

used to determine the flooding velocity [25]. Correlations for non-aqueous absorptions are scarce in literature. Therefore, an aqueous correlation is used in order to estimate the flooding velocity of the gas. The flooding velocity of an aqueous system is estimated can be estimated from the mass transfer area [27].

$$v_{G,F} = \left(\frac{5}{a_g}\right) \ln\left(\frac{2}{3v_L\sqrt{a_g}}\right) \tag{3.18}$$

Once the flooding velocity is determined, the gas velocity is calculated by taking 50 % of from $v_{G,F}$ [27]. An appropriate cross-sectional area of the absorption column can then be calculated. The column's cross-sectional is estimated by division of the liquid flowrate and the liquid velocity. However, since the liquid flowrate is determined by Equations 3.4 and 3.5, the liquid velocity must converge with the estimated flowrate from the mass balances divided by the cross-sectional area.

The final step in the design process is the estimation of the packing height. The packing height is determined based on the desired separation efficiency and the mass transfer characteristics. In the following section a model for estimating the packing height of the absorption column is presented.

3.5.2. Lumped 1D Model of Absorption Column

Modelling packed bed absorption columns in great detail is often difficult for two main reasons. First, the packing of the absorption column is often unstructured and secondly, the gas-liquid interface is often not well defined. Therefore, it is common to use lumped 1D models to describe the system with a limited accuracy. The models can often be improved by correlation from experiments [28]. In this work a lumped 1D model will be used to describe the mass transfer of the system.

Assuming steady state and a constant liquid and gas flow in the column, the CO_2 component mass balances of a slice in the liquid and gas phase becomes.

$$N_z^G y_z A_z - N_{z+\Delta z}^G y_{z+\Delta z} A_z - N_{A,i}^i a_i A_z \Delta z = 0 \tag{3.19}$$

$$-N_z^L x_z A_z + N_{z+\Delta z}^L x_{z+\Delta z} A_z + N_{A,i}^i a_i A_z \Delta z = 0 \tag{3.20}$$

The mass balance is further illustrated in Figure 3.5.

Letting the control volume between z and Δz go to zero, the mole flows is described by two coupled ordinary differential equations (ODEs).

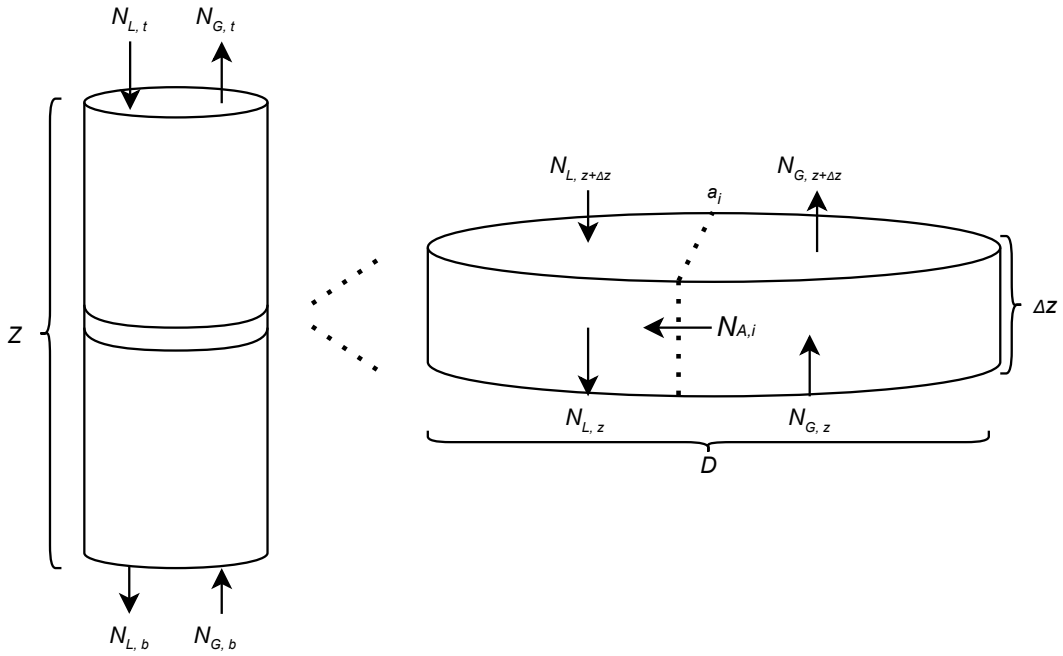

Figure 3.5.: Illustration of ideal component mass balance of a slice in the absorption column.

$$-\frac{dN_z^G y_z}{dz} - N_{A,z}^i a_i = 0 \tag{3.21}$$

$$\frac{dN_z^L x_z}{dz} + N_{A,z}^i a_i = 0 \tag{3.22}$$

Using the two film theory, the mass transport of CO_2, $N_{A,z}^i$, can be described by an overall mass transfer expression

$$N_{A,z}^i = K_G(y_z - y_z^*) \tag{3.23}$$

Since the absorption is enhanced by chemical reactions in the liquid film, the molar fraction at the gas-liquid interface, y^*, is assumed to be far smaller than the gaseous bulk molar fraction, y. Equation 3.23 can be rewritten as

$$N_{A,z}^i = K_G(y_z) \tag{3.24}$$

Combining Equations 3.21, 3.22 and 3.24 obtains the ideal counter current absorption model

$$\frac{dy_z}{dz} = -\frac{a_i}{N_z^G} K_G P_T(y_z) \tag{3.25}$$

$$\frac{dx_z}{dz} = \frac{a_i}{N_z^L} K_G P_T(y_z) \tag{3.26}$$

The change of driving force in the column can then be described by

$$\frac{d(y_z)}{dz} = -\left(\frac{1}{N_z^G} - \frac{H^*}{N_z^L}\right) K_G P_T a_i(y_z) \tag{3.27}$$

By assuming that the flow of CO_2 in the gas phase (N_z^G) is larger than the liquid flow, N_z^L is negligible. By also considering the boundary conditions at the top and bottom of the column, Equation 3.27 can be rewritten.

$$\int_{y_{in}}^{y_{out}} \frac{1}{y_z} d(y_z) = -\left(\frac{1}{N_z^G}\right) K_G P_T a_i \int_0^z dz \tag{3.28}$$

Integration of Equation 3.28 yields the final equation for determining the height of the absorption column.

$$z = \frac{1}{\left(\frac{1}{N_z^G}\right) K_G P_T a_i} ln\left(\frac{y_2}{y_1}\right) \tag{3.29}$$

Equation 3.29 is solved analytically using design parameters from Table B.1 in Appendix B.

3.5.3. Phase Separation Unit

The phase separation in the CCS plant is of high importance because it enhances the concentration of solid particles in the rich stream by separating out a portion of the liquid. When dealing with a hetrogenous or multi-phase mixture, physical separation can be employed by exploiting the differences in densities between the phases [29]. Phase separation is therefore often easier and cheaper than the separation of homogenous mixtures. In this case, a solid-liquid separation is to be carried out, meaning that the solid carbamate salt is to be separated from the liquid.

There are a variety of ways in which phase separations are employed. The principal methods for separation are mentioned by R. Smith [23]. These are

- Settling & sedimentation
- Inertial & centrifugal separation
- Filtration
- Electrostatic precipitation
- Scrubbing
- Floating
- Drying

The most simple devices for separation of hetrogenous mixtures are those that exploit gravitational forces in settling and sedimentation devices. The upward velocity of the fluid in a settler needs to be lower than the terminal settling velocity, v_T, of the particles [23]. Turbulence and high particle concentration has a negative impact on the settling velocity. When this occurs it is called hindered settling [29].

By assuming a spherical particle, an equation for calculating the terminal settling velocity can be derived from the momentum balance of the particle. The steady state momentum balance is derived from the forces acting on the particle. These are the buoyancy force, the drag force and the frictional force [25].

$$\rho_p \left(\frac{\pi d^3}{6}\right) g = \rho_f \left(\frac{\pi d^3}{g}\right) + C_D \left(\frac{\pi d^2}{4}\right) \left(\frac{\rho_f v_T^2}{2}\right) \tag{3.30}$$

Rearranging Equation 3.30 gives the equation for calculating the terminal settling velocity.

$$v_T = \sqrt{\left(\frac{4gd}{3C_D}\right) \left(\frac{\rho_p - \rho_f}{\rho_f}\right)} \tag{3.31}$$

It can be seen in Equation 3.31 that the settling velocity is dependent on the difference in density between the particle and the fluid [30]. It can however be difficult to make estimations of the drag coefficient, C_D. Therefore it is convenient to divide Equation 3.31 into low, intermediate and high regions of Reynolds number [31]. Since the particle size in the slurry is relatively large ($\approx 40\mu m$ [30]) it is assumed that the system has a low Reynolds region.

The low Reynolds number region is described by Stokes' Law

$$F_d = 3\pi\mu v d_p \tag{3.32}$$

Equation 3.32 applies at $Re < 2$, and yields $C_D = 24/Re$ [31]. Applied to Equation 3.31,

it gives the setting velocity of a spherical particle as

$$v_T = \frac{g d_p^2 \left(\rho_p - \rho_f\right)}{18\mu} \tag{3.33}$$

One of the discussed alternatives for performing the heterogeneous separation in this process is lamella sedimentation [30]. Lamella sedimentation is a type of solid-liquid separation process that uses a series of inclined plates or tubes, called lamella (or tube) settlers, to increase the settling area and improve the efficiency of sedimentation.

In lamella sedimentation, the slurry mixture is introduced into a large settling tank or basin, where it flows through a series of inclined plates or tubes that are arranged in a parallel or staggered configuration [30]. The inclined plates are typically made of plastic or metal and have a series of closely spaced channels or corrugations on the surface, which serve to increase the surface area and promote the formation of a thin layer of slurry or solids on the plate surface.

As the slurry flows through the channels of the inclined plates, the solids settle under the influence of gravity and accumulate on the surface of the plate, forming a thick layer or ”sludge” at the bottom of the settling tank. The clarified liquid (or effluent) flows upward and over the top of the inclined plates, eventually collecting in a separate chamber or overflow weir for removal [32]. It should be noted that lamella settlers are typically used for smaller operations and have a suggested maximum flowrate of 20-30 l/s [33]. Therefore, lamella sedimentation is likely a better option for a pilot plant, rather than a full operation.

The terminal settling velocity of particles in the slurry has been determined experimentally from a Master Thesis from 2022 and can be seen in Table 3.4 [30]. The experiment showed that a fully loaded (loading = 0.5) solution of solids at 50 °C resulted in a settling velocity of 80 mm/hr. While this loading is higher than the one used in this work, it is assumed to be the same.

Table 3.4.: Physical properties of carbamate slurry. Data adopted from E. Robertsson[30].
*Extrapolated from other two points assuming linear dependence.
**Approximated value, based on comment in report on drifting experiment.
*** Approximated from 0.5 loading.

Loading	**0.08**	**0,32**	**0.5**	**Unloaded**
Density (g/cmˆ3)	1.06*	1.10	1.12	1.05
Viscosity (mPa/s)	3.51	12**	-	3.51
Concentration of particles (mole/mole)	0.065	0.24	-	0
Settling vel. (mm/hr)	6.35	80***	80	0

Inertial or centrifugal separators could be used in order to decrease the needed size of the phase separator. The terminal radial velocity, $v_{T,r}$, is the velocity of the particles influenced by centrifugal forces. It is calculated for a unhindered particle that follows Stokes Law [34], by modifying Equation 3.31, where the gravitational acceleration, g, is replaced by centrifugal acceleration, $R\omega^2$

$$v_{T,r} = \frac{R\omega^2 d_p^2 \left(\rho_p - \rho_f\right)}{18\mu} \tag{3.34}$$

Centrifugal separations are, however, much more expensive, since they need electricity to be operated. Therefore, this work will only estimate an area for a simple sedimentation tank with the objective of thickening the slurry - a thickener. It is worth noting that the settling area will be large with this method. Ways to decrease the sedimentation area are included later in the discussion.

A thickener is an industrial device used to increase the concentration of particles through sedimentation, resulting in the formation of a clear liquid [35]. Thickeners can operate continuously or in batches and consist of tanks that remove the clear liquid from the top and the thickened slurry from the bottom [31].

To achieve the maximum throughput possible from a given thickener size, sedimentation rate should be as high as possible. Electrolytes or poymers can be added in small amounts to increase the rate of sedimentation artificially by causing the precipitation of colloidal particles and the formation of flocs [35]. Frequently, the suspension is heated to lower the viscosity of the liquid and encourage larger particles in the suspension to grow at the expense of smaller, more soluble ones [35]. Additionally, the thickener often contains a slow stirrer, which reduces the apparent viscosity of the suspension and aids in sediment consolidation [23].

The continuous thickener consists of a cylindrical tank with a flat bottom. The suspension is fed in at the centre, at a depth of from 0.3 to 1 m below the surface of the liquid, with as little disturbance as possible. The thickened liquor is continuously removed through an outlet at the bottom, and any solids which are deposited on the floor of the tank may be directed toward the outlet by means of a slowly rotating rake mechanism [35]. An illustration of a thickener can be seen in Figure 3.6.

As can be seen in Figure 3.6, the function of the thickener is two-fold. It must, firstly, produce a clarified effluent, and must therefore at all times have an upwards velocity of the liquid lower than the settling velocity of the solids. Secondly, the thickener also must produce a more concentrated slurry in the suspension [35]. Consequently, there are two distinct design criteria of a thickening unit. The diameter must be adequately large in order to produce a clarified liquid, while the height of the governs the degree of thickening of the concentrated slurry. In this work the area is the only one investigated.

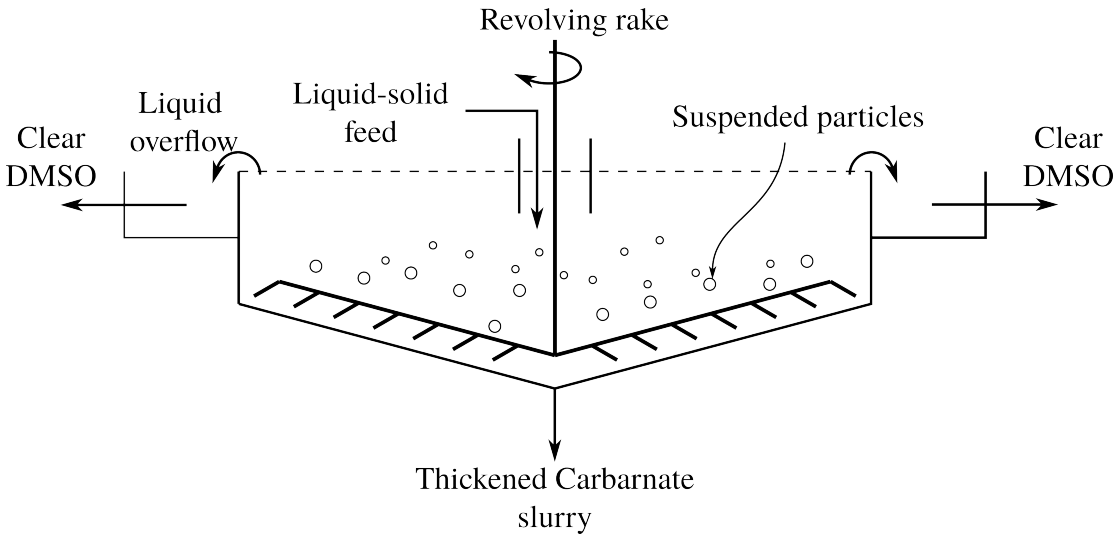

Figure 3.6.: Illustration of a thickener used in the process. Adopted from R. Smith [23].

3.5.4. Size Estimation

The following section describes the method used to estimate the size needed for the thickener. In the mass balance calculations, it was assumed that 90 % of the liquid is separated in this unit. The liquid overflow is purely liquid and the underflow has a larger concentration of the carbamate salt in 10 % of the liquid.

By assuming that all CO_2 in the fluid is precipitated and that the amount of precipitated AMP follows Reaction 2.3, it is possible to estimate the amount of solids in the feed stream. The mass flow of solids in the feed stream to the thickener is

$$F_s = (F2_{CO2} + 2 \cdot F2_{CO2}) \tag{3.35}$$

where F_s is the mass flow of solids and $F2_{CO2}$ is the mass of CO_2 in stream F2 in Figure 3.3. The liquid mass flow (F_l) can then easily be calculated by subtracting the total mass of the stream ($F2$) with the mass of solids.

$$F_l = F2 - F_s \tag{3.36}$$

The area of the thickener can be estimated by knowing the design requirements and the liquid-to-solid ratios in the feed and the thickened slurry. The liquid-to-solid ratio is found by the ratio of Equations 3.36 and 3.35. The liquid-to-solid ratios in the feed and the thickened outflow (or underflow) is denoted Y and U respectively. The required area for a specified separation can then be calculated [35].

$$A = V_0 C_s \rho_s \frac{(Y - U)}{v_T \rho} \tag{3.37}$$

where V_0 is the volumetric feed flow, C_s is the solid concentration, ρ_s is the density of solids and ρ is the density of the solution. ρ_s is not determined experimentally. The product of V_0, C_s and ρ_s is the mass flow of solids in the feed, which is known from Equation 3.35. Equation 3.37 can then be rewritten by making the following substitutions.

$$A = F_s \left(\frac{\left(\frac{F_l}{F_s}\right) - \left(\frac{0.1F_l}{F_s}\right)}{v_T \rho} \right) \tag{3.38}$$

Equation 3.38 is then solved in order to estimate the sedimentation area of the thickener.

As mentioned, the thickener is likely to have a large area due to both the amount of liquid separated and the relatively low v_T. Sensitivity analysis is made on this unit where amount of liquid separated is lowered in order to investigate the impact on size and heat demand in the desorption unit due to more liquid mass being fed to the evaporator. Furthermore, v_T can be increased by various methods. An additional sensitivity analysis of the v_T effect on the thickener area is therefore made.

3.5.5. Desorption Unit

The next step in the process is the desorption unit. In the desorption unit, sufficient heat must be applied in order increase the temperature of the slurry to 88 °C and also to reverse the absorption reactions (Equation 2.3 and 2.4).

$$Q_{tot} = Q_{sens} + Q_{des} \tag{3.39}$$

The pilot plant utilizes a desorption tank in the form of stirred tank reactor for the desorption (H. Svensson 2023). This unit is suitable for a pilot plant due to its simplicity, however it offers limited heat and mass transfer area. Therefore, a more suitable unit of operation at a scaled up plant would be an evaporator.

Evaporators are devices that are used to remove liquid from a solution or mixture by converting it into vapor [36]. They work based on the principle of heating the solution to increase its temperature above the boiling point of the liquid component, causing it to evaporate and leave behind the solid or concentrated liquid components [29]. Evaporators are typically comprised of a heat exchanger, which is used to transfer heat from a heating medium to the incoming stream to increase its temperature. As the temperature of the stream increases, the liquid component begins to boil and form vapor, which is then

separated from the solid or concentrated liquid components using a separator.

There are several types of evaporators, including falling film, rising film and thin film evaporators. The type of evaporator used depends on the properties of the incoming stream and the desired evaporation rate [36]. Thin film evaporators are suitable for medium-to-high viscous solutions but requires more detailed design and are not suitable for large flows [23]. Therefore, a single stage rising film evaporator will be used for a rough estimation of the design [26].

One of the key factors affecting the efficiency of an evaporator is the overall heat transfer coefficient (k), which is a measure of the rate at which heat is transferred from the heating medium to the incoming stream. This is influenced by factors such as the type of evaporator, the flow rate of the incoming stream, and the design of the heat exchanger [36].

The heat transfer area required for the evaporator is estimated based on the overall heat transfer coefficient, the total heat duty and the logarithmic mean temperature difference ΔT_{log} between the heating medium and the incoming stream [37]. The heat transfer area needed is therefore

$$A_h = \frac{Q_{tot}}{(k \cdot \Delta T_{log})} \tag{3.40}$$

where ΔT_{log} is defined as

$$\Delta T_{log} = \frac{\Delta T_1 - \Delta T_2}{\ln\left(\frac{\Delta T_1}{\Delta T_2}\right)} \tag{3.41}$$

The value of k is unknown for this configuration and needs to be approximated. Typical values for k for falling film evaporators range between $1000 - 4000 W/m^2K$ [36]. Since the use of hot water (instead of steam) as heating medium could have a negative impact on the k value due to lower specific heat capacity [22], k is assumed to have the value of $1000\ W/m^2K$.

3.6. Cost Estimations

This section covers the methods used in order to make the cost estimations on the direct capital expenditure (CAPEX) of the carbon capture plant. Literature sources for carbon capture plants using MEA technology are available and are used to make a comparative reference case.

3.6.1. Reference Case

A research article published in American Chemical Society in 2018 is used as a reference for this estimation [38]. The research paper investigates the effect of partial capture, meaning the reduced capture rate of CO_2, on specific capture costs. The article investigates the use of partial capture as a measure to decrease the total CAPEX of a CCS plant, and thereby the risk of investment. It compares two path ways for partial capture. These are defined as the separation rate path(SRP), where only a fraction of the CO_2 is separated from the full flue gas stream, and slip stream path, where only a fraction of the flue gas stream enters the CCS plant [39].

Comparisons are made on the input data used in this work and the reference case. This is seen in Table 3.5. The reference case full captured is specified with a CO_2 concentration of 20 vol% and a flow rate of 200 kg/s at 150 °C and pressure of 1 bar. The flow rate is more than twice as large in the reference case than the one studied (Table 3.1). However, the slip-stream analysis is based on 60 % of the flue gas flow rate being directed to the CCS plant. This results in a flow rate of 120 kg/s, which is still larger. The increased CAPEX due to larger flow rate is however likely to be counter-acted by the higher CO_2 concentration because both these parameters have an impact on the absorption design [40]. From Table 3.5, it is estimated that this work is comparable to the 60 % SSP case.

Table 3.5.: Input data for full capture, 60 % separation rate path (SRP) and for 60 % slip-stream path (SSP) reference case in comparison to this work. Reference data adopted from M. Bierrmann et.al [38].

	This Work		**Ref. Full (SRP)**		**Ref. SSP**	
Property	**Value**	**Unit**	**Value**	**Unit**	**Value**	**Unit**
Mass flow	65	kg/s	200	kg/s	120	kg/s
Temperature	45	^{o}C	150	^{o}C	150	^{o}C
CO2	13	Vol%	20	Vol%	20	Vol%
Capture rate	90	Mol%	90 (60%)	Mol%	90	Mol%

The capital cost estimation made by M. Bierrmann et. al includes the entire capital expenditure of a MEA capture plant [38]. The capital costs are divided in to 5 categories, these are columns, heat exchangers, fan & compressors, pumps and other vessels and filters. The cost is also allocated to the different main parts of the process. These are the absorption, desorption, direct contact cooler, reclaimer, reboiler, compressor and other. The total CAPEX

It is noted that this cost estimation in Figure 3.7 is based on a more detailed process flowsheet. Most of the investigated equipment are outside the scope of this thesis. Furthermore, some of the equipment are needed specifically for the MEA process.

From Figure 3.7, it is observed that the total CAPEX of the reference case is 93 million €. 22 million is allocated to the columns of which 11 million is due to the absorption, 5

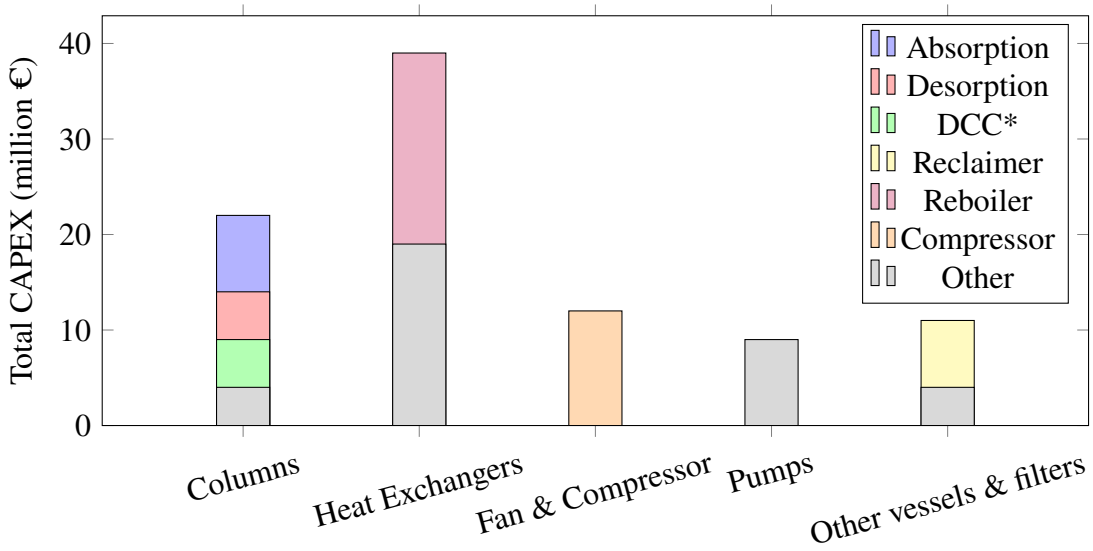

Figure 3.7.: Detailed equipment costs for for a aqueous MEA plant designed for 90% capture of CO_2. Adopted from M. Biermann et.al.[38].
Note: *DCC - Direct Contact Cooler for cooling of the hot flue gas stream before absorption.

million each to the desorption and DCC and 4 million allocated to other columns. The heat exchangers are the most costly type of equipment with a toal cost of 39 million €. More than half of the heat exchanger CAPEX is allocated to the reboiler in the desorption unit (20 million €). The rest is split between the various heat exchangers in the process. It is estimated that half the rest of the heat exchanger CAPEX is outside the scope of this thesis, due to a lot of these being part of the liquefaction process of the captured CO_2 [39]. Fan & compressor units is estimated at 12 million, of which it is estimated that all is allocated to the compressors in the liquefaction [38]. Pumps are estimated at 11 million €, of which all are within the scope of this thesis. The reclaimer is a unit that is usually required in MEA processes. The purpose of this equipment is mainly to eliminate any degradation products [41]. While AMP/DMSO system is likely to require similar equipment it is deemed to be outside the scope of this thesis.

By only including the relevant equipment within the scope of this thesis, Figure 3.7 can be redrawn. The CAPEX of comparable units are viewed in Figure 4.3. The total CAPEX of comparable units in the reference case configuration is 52 million €.

3.6.2. CAPEX of System-Specific Equipment

Some of the equipment in the AMP/DMSO system can be approximated to have simliar costs as the reference MEA system. These include the absorption column, most heat exchangers and pumps. Some units are, however, specific to the non-aqueous system. These are not included in the reference case and must be estimated separately.

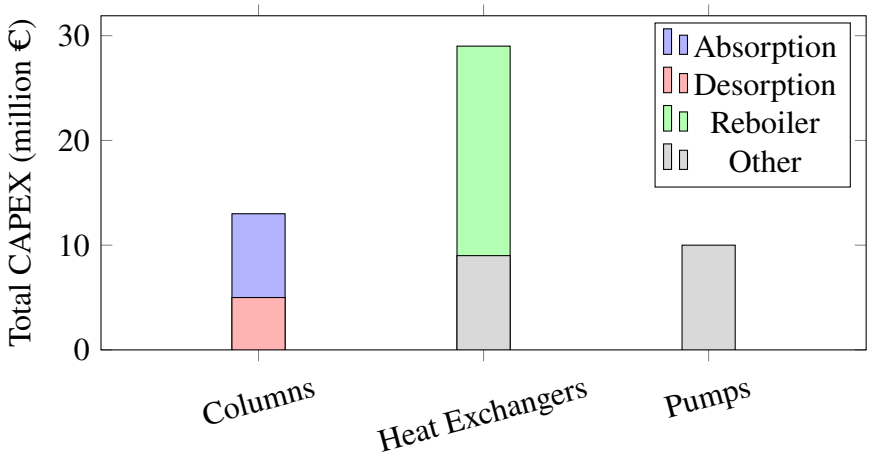

Figure 3.8.: Detailed equipment costs for relevant equipment to this work. Equipment that has been neglected are due to either not being within the scope, or being specific equipment to the MEA process and therefore not needed in this process configuration.

The equipment that needs to be included is:

- The Sedimentation Tank
- The Evaporation Column
- The Reboiler

The cost analysis is conducted by taking into account the outcomes of the preceding dimensioning calculations and the requisite utility usage for the process model. Subsequently, the capital costs for the plant are estimated. The calculations are carried out using correlations in literature. Specifically using in Chemical Process Design and Economics by G.Ulrich [26]. The price of the equipment is based on the CE Plant Cost Index 400 (January 2004) and must therefore be adjusted for inflation. In this work, annual inflation rate (I_r) of 2 % is used for this estimation [42]. The adjusted price (p_{adj}) is then calculated from the original price (p_o).

$$p_{adj} = p_o \left(1 + i_r^{(2023-2004)}\right) \tag{3.42}$$

3.7. Sensitivity Analysis

Three scenarios are investigated for three uncertain parameters. The scenarios are denoted S1-S3. The scenarios are:

- S1: Influence of lower absorption heat on the energy demand

- S2: Effects of lower liquid overflow in thickener on energy demand and thickener area
- S3: Effects of larger particle diameter on thickener area

These scenarios are described and justified in the following subsections.

3.7.1. S1: Influence of Absorption Heat on the Energy Demand and Evaporator size.

The heat of absorption has been determined experimentally, seen in Table 3.2. The ΔH_{abs} is highly dependent on temperature and get lower at higher temperature [13]. The value of ΔH_{abs} at 50 °C was used for both the absorption and the desorption. The desorption heat has not been investigated by researchers, therefore the same value was used for the desorption and absorption. However, it is possible to argue that the desorption heat is lower than the absorption heat due to higher temperature. That is why in this scenario ΔH_{abs} at 88 °C is used in order to see how that effects the energy demand of the desorption column. The ΔH_{abs} at 88 °C is 70 kJ/mole CO_2 as opposed to 115 kJ/mole CO_2 used previously.

Equations 3.12 and 3.39 are applied to new value in order to see the effects on the energy demand. Equation 3.40 is used to estimate the new size of the evaporator.

3.7.2. S2: Effects of Liquid Overflow in Thickener on Energy Demand and Thickener Area

In the design equation of the thickener (Equation 3.38) it is observed that the required sedimentation area of the thickener is highly dependent on the separation efficiency. The ratios of solids and liquids in the feed (U) and underflow (Y) is expressed as F_l/F_s. In the mass balance calculations, the phase separator was assumed to separate 90 % of the liquid with no particles in the liquid overflow. Since the v_T of particles in the slurry is slow, a 90 % separation of liquid is likely to cause a large area of the thickener. The separation efficiency is therefore altered to investigate the changes this has on the thickening area, at the expense of a higher energy demand due to less mass being separated.

Assuming that the separation efficiency is lowered to 60 % liquid separation, the mass balance of the thickener is expressed as

$$F2 = F3 + F4 \tag{3.43}$$

where F4 is the mass flow of the underflow and equals the solid particles and 40 % of the liquid.

$$F4 = F_s + 0.4F_l \tag{3.44}$$

The U term in Equation 3.37 is then rewritten to $U = \frac{0.4F_l}{F_s}$, which is substituted in to Equation 3.38, yielding the following design equation for the thickener.

$$A = F_s \left(\frac{\left(\frac{F_l}{F_s}\right) - \left(\frac{0.4F_l}{F_s}\right)}{v_T \rho} \right) \tag{3.45}$$

The increase of mass flow in F4 has an impact on the rich-lean heat exchanger and the desorption unit. Energy balances are therefore made by substituting the mass flow in Equation 3.9, with the one determined by Equations 3.43 and 3.44 in this analysis.

3.7.3. S3: Effects of Particle Diameter on Thickener Area

Particle diameter has a large influence on v_T, according to Equation 3.33. As mentioned, v_T was determined experimentally. There are however reasons to suggest that the v_T could be larger in this process configuration.

In the experiments on the particle diameter, made by E. Robertsson, particles were observed in the overflow (or *Effluent flow*) of the sedimentation tank [30]. In this process configuration, this means that particles will be recirculated to the absorption column through streams F3 and F9 in Figure 3.3. If particles are fed to the absorption column, the crystallization occurs much faster [12]. It is therefore likely that the mean particle diameter is going to be larger which would impact the settling velocity positively in accordance with Equation 3.33.

In this scenario, the final area is estimated based on a diameter that is twice as large. Assuming all other parameters remain constant the settling velocity (v_T) can be extrapolated from the experimentally determined velocity in Table 3.4 (now denoted v_{T0}).

$$\frac{v_T}{v_{T0}} = \frac{d^2}{d_0^2} \tag{3.46}$$

If the diameter corresponding to the extrapolated v_T is twice as large, it can consequently be calculated as

$$v_T = \frac{(2 \cdot d_0)^2}{d_0^2} v_{T0} \rightarrow v_T = 4 \cdot v_{T0} \tag{3.47}$$

Equation 3.47 can then be used in order to estimate the new area of the thickener by substituting v_T in to Equation 3.38.

Chapter 4.

Results & Discussions

This chapter presents the main results from the methods used in the previous chapter. The mass and energy balances are available in its entirety in Appendix A.

4.1. CO_2 Capture and solvent use

Capturing 90 % of the CO_2 in the flue gas at Örtofta power plant means that there will be a capture rate of 40 tonnes per hour of operation. Considering that the plant is operated at full capacity 180 days each year[19], that results in an yearly production of 172800 tonnes of captured CO_2.

Table 4.1.: Mass flows of absorbent solutions per second and levelized to amount of CO_2 captured.

Component	Mass Flow Rate	
	kg/s	kg/kg CO2
AMP	82	7.4
DMSO	247	22.2

4.2. Energy Demand

Figure 4.1 displays the energy demands, measured in MW, of the AMP/DMSO system applied to the flue gas stream. The demands include total heating, total cooling, and heat recovery. The heating demand of this technology is 19 MW. The cooling the demand is 39 MW. The heat recovery in the rich lean heat exchanger is 8.47 MW. The cooling demand is largely due to the internal cooling of the absorption unit in order to keep the absorption at a stable temperature. The heating demand is mostly due to the reboiler duty of the desorption unit.

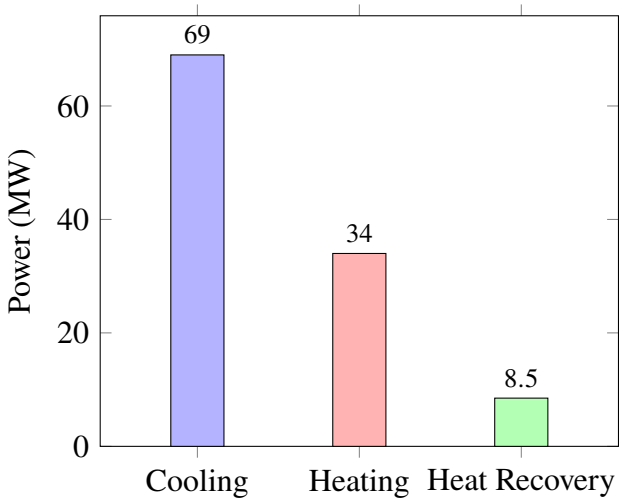

Figure 4.1.: Power distribution of the system

A common way of comparing carbon technologies efficiency is in the form of MJ/CO_2 captured. In Table 4.2, this has been calculated for the AMP/DMSO system and is listed with figures listed in literature [11], [40], [43]. Also included in Table 4.2, is the estimated value from a separate report made on a CCS plant applied to Örtofta Power Plant by Captimise Consulting. The report does not mention a specific system for the carbon capture. The efficiency of the AMP/DMSO system is calculated to 3.07 MJ/kg CO_2. Values for the conventional MEA technology found in literature varies between 3.57-4.0 MJ/kg CO_2. The captimise report mentions an efficiency of 2.44 MJ/kg CO_2 of the unspecified ”enhanced amine technology”. Both the comparative amines needs low pressure steam as stripping agent, while AMP/DMSO is heated by the district heat streams.

Table 4.2.: Comparative results of the AMP/DMSO reboiler efficiency with other calculated as MJ/Kg Captured CO_2.
*Captimise has made an assesment based of 2.44 efficiency of an unspecified ”enhanced amine” technology.

Technology	**AMP/DMSO**	**MEA/Water**	**Enhanced Amine***
Efficiency	3.07	3.57-4.0	2,44
Heat source	DH	LP Steam	LP Steam
Source	This study	[11], [40], [43]	Captimise report*

Since the AMP/DMSO investigated has a higher efficiency than the one investigated by Captimise, the heat required to operate the CCS fascility is higher for each amount of CO_2 captured. However, since both reference cases needs LP steam to operate, this will account for a direct loss of electricity or power production of the plant [38]. Because Kraftringen AB are unlikely to have the capacity of lower production, the direct loss of power production are going to be compensated by an increase in fuel burning. In other

words, more CO_2 is needs to be produced in order to capture the CO_2. In the case of AMO/DMSO, this direct loss of power is not as apparent.

The amount of heat transfer and other properties regarding the heat exchangers within the system are listed in Table 4.3. HEX 1 and 3 requires 8-10 MW of 10 and 30 °C cooling utility respectively. The cooling utility needs to be supplied by a heat pump, since the return temperature of the DH is too high (Table 3.3). HEX 2 requires 50.9 MW of cooling. Assuming that the heat exchanger used allows for a ΔT_{MIN} of 8 °C and that the average heat of the returning DH is kept at 42 °C, the cooling can be supplied directly from the returning DH. HEX 4 in the desorption unit requires 34.2 MW of heating medium. By assuming a ΔT_{MIN} of 8 °C, the outgoing temperature of the heating utility is calculated to 82 °C. This suggests that the desorption unit can be operated directly by the DH stream produced by Örtofta CHP plant at the the expense of lowering the temperature to 82 °C. According to Martin Petersen at Kraftringen AB, a product stream of 82 °C is sufficient in order to meet the consumer heating demand in the DH network (From conversation with M. Petersen, March 2023).

Table 4.3.: Heat transfer in heat exchangers (HEX) and temperatures of the cooling and heating utility streams. Abbreviations of "Utility Streams" are taken from Figure 3.3.
*The average temperatures of the DH and the returning DH from Table 3.3.

HEX #	Heat Transfer	Cooling/Heating	Utility Stream	T_{in} (°C)	T_{out} (°C)	Source of Utility
1	8.1 MW	Cooling	C1	10	<25	Heatpump
2	50.9 MW	Cooling	C2	42*	60	Return DH
3	9.8 MW	Cooling	C3	30	<50	Heat pump
4	34.2 MW	Heating	H1	97*	82	DH

4.2.1. Matching Available Heat with Energy Demand

The available heat in the DH and returning DH is viewed in Table 4.4. It is estimated that 47.3 MW of cooling utility is available for the cooling of the absorption column and 30.6 MW of heating utility is available for the desorption column.

Table 4.4.: Available heat in the DH and returning DH streams from Örtofta CHP plant estimated by changing the average temperatures in Table 3.3 (T_1) to the outgoing temperature (T_2) using Equation 3.9.

Stream	$T_1 \rightarrow T_2$	Q (MW)
DH	97 → 82	30.6
Return DH	42 → 65	47.3

From Table 4.3 and 4.4 it is possible to examine the heat integration possibility of the proposed CCS plant. Internal utility is used to describe the heat that is recovered directly

from the outgoing DH and returning DH streams. External is used to describe the heating and cooling needed from additional heat pumps. The design of the heat pump are not included in this work. A histogram of the internal and external utilities is viewed in Figure 4.2. The amount of internal utility is a total of 82 MW. The external cooling utility needed is 22 MW. The external heating utility is 4 MW.

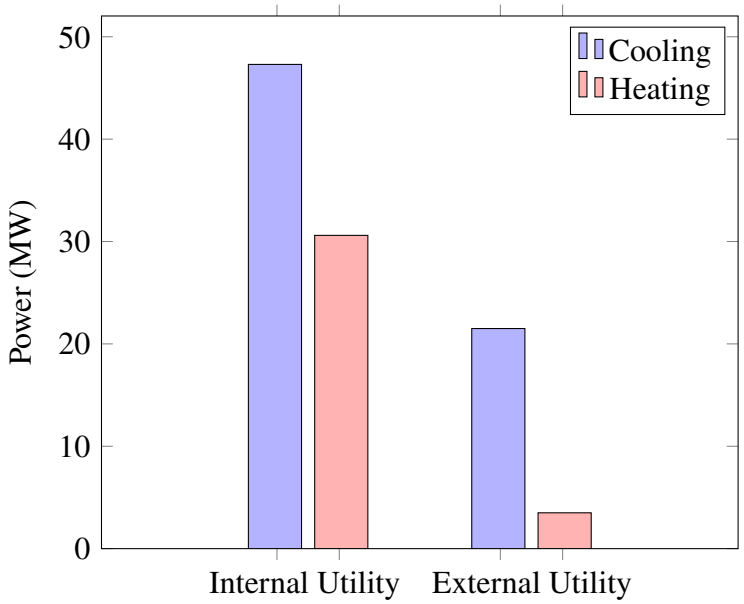

Figure 4.2.: Internal and external utility needed for the operation of the CCS plant. Internal utility means that the power is taken directly from the district heating outflow stream or returning stream. External Utility is power that needs to be supplied from heat pumps.

As seen in Figure 4.2, the DH streams from Örtofta CHP plant is not able to meet the entire energy demand of the proposed CCS plant configuration. This estimation is based on various assumptions that might affect the results. Furthermore, the average flowrate and temperature of the DH (Table 3.3) is varying substantially on a yearly basis. This will affect the amount of available heat. Further analysis on the available heat needs to be done. Careful considerations regarding the heat exchanger designs could improve the heat transfer and make it possible for a heating supply that meets the demand completely. The cooling demand is however unlikely to be met due to the temperatures needed in HEX 1 and 3, seen in Table 4.3. These amounts to 18 MW which will need to be supplied by the addition of heat pumps. HEX 2 could be improved in order to be fully operated by the returning DH stream by a relatively small increase in efficiency.

The heat transfer in HEX 2 will raise the temperature of the returning DH stream to 65 °C. There might be additional issues in raising the temperature of the returning DH stream. The implications of this needs further assessment.

4.3. Equipment Results

The equipment within the project is split between primary and secondary equipment. The primary equipment includes the absorption column, evaporator and thickener. The secondary equipment includes the pumps and the heat exchangers in the system.

The equipment sizes of the primary equipment are listed in Table 4.5. The absorption column will have cross sectional area of 79 m^2, and a total height of 15 m, of which 10 m are packing. The evaporator is calculated to have a heat transfer area of 2500 m^2. The thickener requires an area of 10000 m^2 and a diameter of above 300 m.

Table 4.5.: Equipment sizes for the AMP/DMSO primary equipment - Absorption, Evaporator and Thickener.

Absorption Column				**Evaporator**	**Thickener**	
Area (m^2)	Diameter (m)	Packing height (m)	Total height (m)	Heat Transfer Area (m^2)	Area (m^2)	Diameter (m)
79	10	10	15	2500	10000	120

The absorption column is considered to be reasonable in size. When comparing with other studies it is apparent that most calculated absorption columns are in the range of 10-20 m high [11][38][40]. When looking at the design equation for the height of the absorption column, Equation 3.29, it is apparent that the height is strongly dependent on the driving force of the mass transfer. A higher concentration of CO_2 in the flue gases, means that the column would be less high. If height restrictions are limiting it could be possible to increase the CO_2 concentration further by a pre-filtration step before the absorption. Another way is to operate the absorption at a higher pressure by installing a compressor previous to the absorption. The cross sectional area of the column is highly dependent on the flow rate of the flue gases. If the area is limiting, it would be preferred to limit the flow rate through a slip stream separation path (SSP), by only leading a portion of the flue gases to the CCS plant [38].

The evaporator is calculated to have a heat transfer area of 2500 m^2. The type of evaporated is estimated as a single stage rising film evaporator. Rising film evaporators accommodates larger heat transfer area than falling film evaporators [36]. One viable alternative is also to couple a multi-stage falling film evaporator, where multiple units are coupled in series. This is a common practise in process industry as the gas stream from one evaporator can be used to heat the next one which often leads to substantial energy savings [23]. Since the desorption step is the least investigated unit in the AMP/DMSO process, further considerations must be taken when designing this unit.

While both the absorption column and the evaporator are estimated to have reasonable equipment sizes, the thickener is estimated to be, by far, bigger than what can be accomodated. The reason for the large size of this process equipment is due to both process specifications and properties of the slurry. The separation requirement in the

mass balance calculations was assumed at 90 % separation of liquid DMSO. When observing the design equation of the thickener (Equation 3.38), it is apparent that the area is highly dependent on the liquid-to-solid ratios (F_l/F_s) in the feed and the thickened underflow. Sensitivity analysis on this parameter is therefore done in order to investigate of much impact this will have on the total design of the thickener.

A relatively large area of the thickener is, however, still expected due to the settling velocity of particles in the slurry, v_T, being slow. This property was determined experimentally using different different loadings and temperature [30]. Equation 3.33, describes the properties affecting the settling velocity of particles. Here it is apparent that the size of the particles have a large impact on the settling velocity. In the experiment made by E. Robertsson, it is seen that the size distribution of the particles are relatively high. They might also be estimated to be smaller than they going to be in a pilot plant or full scale operation. M. Sanku mentions in her dissertation from 2021, that the crystallization kinetics of the carbamate salt are very slow. However, if they are already present in the feed the particles grow much faster in size [12]. This means that if particles are present in stream F9 in Figure 3.3, the formation of larger particles is induced. This is considered likely, due to the relatively slow v_T. In sensitivity analysis S3, this is investigated further.

4.4. Capital Expenditure Estimation

The design specifications of the primary equipment in Table 4.5 are used in equipment cost correlations listed by G. Ulrich et. al [26]. The absorption column is estimated to have the same cost as the refernce case. The thickener and the evaporator original price and adjusted price is viewed in Table 4.6.

Table 4.6.: Original purchase cost, p_o, and adjusted purchase cost for inflation, p_{adj}, estimated for the evaporator and thickener in the process.

Evaporator		Thickener	
$p_o \cdot 10^{-6}$	$p_{adj} \cdot 10^{-6}$	$p_o \cdot 10^{-6}$	$p_{adj} \cdot 10^{-6}$
4.34	10.6	15	36.8

With the addition of the Thickener and Evaporator units, Figure 3.7 is redrawn. The equipment that is used for desorption in the reference case (Reboiler and Desorption Column) is substituted by the estimated Evaporator column. The thickener is not needed in a MEA Process and is added without substituting any other costs. The CAPEX of comparable equipment for the AMP/DMSO process is viewed in Figure 4.3.

From the CAPEX of equipment in Figures 3.7 and 4.3 it is possible to compare the direct equipment costs. This is summarized in Table 4.7. The AMP/DMSO is more expensive to build than the reference MEA process. The reason for this is mainly due to the

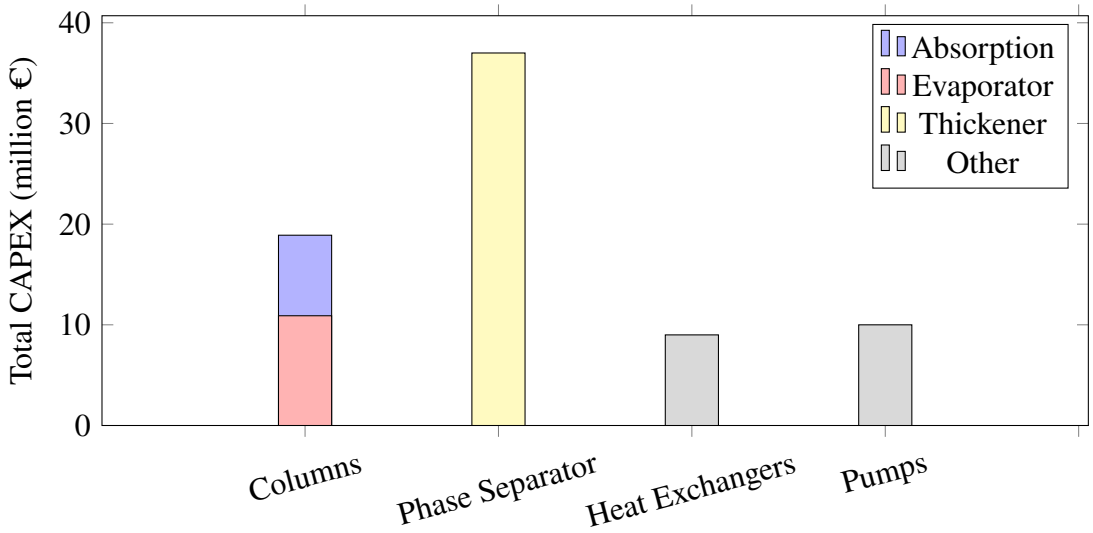

Figure 4.3.: Detailed equipment costs for relevant equipment to this work. Evaporator and Thickener has been estimated from correlations.

addition of the phase separator (thickener) to the process configuration. The absorption columns for both cases are estimated to 8 million €. The desorption are estimated to 10.6 and 25 million € respectively. Other equipment are estimated to 46 and 19 million €. The reason why the desorption is more expensive for the reference case is due to the large reboiler that is needed to drive the stripping column in a MEA process. Since the desorption column in the AMP/DMSO can be operated by the district heat, it is assumed that the heat transfer is directly integrated in to the evaporation column. The AMP/DMSO process has a higher total CAPEX than the reference case. This is mainly due to the thickener, which allocates 37 million €.

Table 4.7.: Comparative CAPEX assessment between this work and reference case. Adopted from Figures 3.7 and 4.3. The equipment are grouped in the three categories; absorption desorption and other.

Category	**This Work (million €)**		**Reference Case (million €)**	
Absorption	Column	8	Column	8
Desorption	Evaporator	11	Column Reboiler	5 20
Other	Thickener Other	37 19	Other	19
	Total	**75**	**Total**	**52**

4.5. Sensitivity Analysis

The summarized results of the three scenarios of the sensitivity analysis is presented in Table 4.8. Each are discussed in the following paragraphs.

Table 4.8.: The results of S1-S3, where parameters from equipment design equations are varied to see the effects on the process as well as the CAPEX reductions.
Base: Q_{tot}=34 MW, A_h=2500 m^2, A=10000 m^2, CAPEX=75 million €

	Scenario	Variance	Effects	CAPEX
S1	Absorption Heat	$115 \xrightarrow{\Delta H_{abs}} 70$	Q_{tot}: -12 MW A_h: -900 m^2	-3.1 million €
S2	Liquid Overflow	$\frac{0.1F_l}{F_s} \xrightarrow{U} \frac{0.4F_l}{F_s}$	Q_{tot}: +2 MW A: -3300 m^2	-29 million €
S3	Particle Diameter	$2d_0$	A: -7500 m^2	-32 million €

The value of ΔH_{abs} is substantially lower at a temperature of 88 °C [13]. The heat generated by the absorption reactions are directly proportional to ΔH_{abs}, which in turn is used to estimate the heat needed for desorption. The heating demand of the desorption (Q_{tot}) is lowered substantially. From the original estimation this was 34 MW, but is now lowered to 22 MW. The size of the evaporator is also dependent on the desorption heat, according to Equation 3.40. The decrease in Q_{tot} has the effect of lowering the evaporator size from 2500 m^2 to 1600 m^2. Another effect is that the heat available in the DH stream is enough to operate the desorption.

Arguments can be made for both scenarios. Since experiments of absorption heat has been conducted for 88 °C it suggests that the desorption heat at this temperature should be equal or at least close to this value. On the other hand, the overall energy balance needs to be reconsidered if this is true. If less energy is required for desorption than absorption, the difference in input and output of energy must be compensated by something else, in accordance with the first law of thermodynamics [44]. The desorption heat needs to be experimentally determined in order to validate these assumptions.

Changing the separation efficiency in the thickener by lowering the amount of liquid overflow, lowers the required area by -3300 m^2. The effects that the lower separation has on the energy demand is 2 MW.

Minimizing the space needed for the thickener is essential. How much that can be decreased at the expense of higher energy demand needs to be carefully calculated.

From Table 4.8, it is seen that the area of the thickener is very sensitive to particle diameter (d). This is because the v_T is four times faster when d is twice as large. Since the area is reciprocally proportional to v_T (Equation 3.38), the required area is four

times smaller in this scenario. The validity of this needs to be further considered by tests on a pilot facility. As mentioned in Chapter 3, there are ways of increasing the v_T, either by centrifugal or inertial forces, or by induced flocculation of particles [35]. The main advantage of a thickener is that it is vary simple process equipment and that operates purely on gravitational forces. However, if space-requirements are limiting, other equipment options should be considered, as more advanced equipment generally takes up less space.

It is apparent that both physical properties (such as absorption heat and particle diameter) as well as changes in process configurations has a high impact on the energy demand and the equipment dimensions. These in turn also have a large impact on the CAPEX of the process. S1 leads to a smaller evaporator and results in -3.1 million €. S2 and S3 leads to a smaller thickener and saves 29 and 32 million € respectively. It should be noted that these are estimations made from correlations in literature that might not be up to date. It does, however, illustrate the importance of process design and indicates that the process can be optimized further.

4.6. Uncertainties

The simplification of calculations and the reliance on assumptions have implications for the accuracy of the results obtained in this study. Assumptions introduce uncertainties that can impact the results to varying degrees. This section will discuss the most important uncertainties and their impact on the process.

One such assumption is that no water is absorbed into the carbon capture systems from the flue gases. AMP/DMSO is modelled as a water-free system and the presence of water in the feed might impact the system. Water from the flue gases can be absorbed in the solution, leading to an increased formation of bicarbonate, which in turn affects the precipitation of carbamates [13]. Furthermore, there is a risk of increased heat demand in the desorber due to the higher regeneration temperature required for bicarbonate compared to carbamate, and the possibility of water evaporation, which consumes energy. While studies on water-lean absorption systems have shown high tolerance for water when the water load reaches a steady-state during operation [45], further investigation is needed to understand the extent of water accumulation and its effects on the AMP/DMSO system before assessing the influence of added water.

Another set of assumptions are in regards to the available heat in the DH streams. In Table 3.3, the temperature of the streams have a relatively high variance. The temperature of these streams strongly affect the energy available for the CCS plant (Table 4.4). The implications of the varying temperatures to the system needs to be considered. Once these are established, measures should be taken to ensure a more steady temperature variance. The same argument is made for the flowrate of the DH. In this work, an average flow rate is considered. However, the internal reporting system at Kraftringen suggests

that this can vary by ±400 m^3/hr. This has the error of roughly ±7 MW of available heat in by the DH stream and roughly ±10 MW in the returning stream.

DMSO has a high boiling point of nearly 200 °C [46]. The output stream from the CCS plant is still likely to contain some amount of DMSO. This might effect the proposed planning of the plant because organic solvents needs to be treated more rigorously than water, in accordance with regulation (2013:254) on emission of volatile organic substances (VOC). How much DMSO that evaporates must be determined at a pilot plant to ensure that it can be handled appropriately.

The presence of NO_x in the flue gases are significant issue for any carbon capture plant that utilize an amine aborption system. The reason is that these substances react with the amine, forming toxic N-nitrosamines. In order to apply this system, it must be ensured that the amount of NO_x in the flue gas is kept under a certain limit [20]. The N-nitrosamines can be mitigate by electrochemical reduction if they are present in the emissions of the plant. It has been introduced as an option to drastically reduce the amount of N-nitrosamines from a emission control system at a CCS plant [21].

Although the individual effects of most assumptions and simplifications are relatively small, their cumulative impact should not be overlooked. However, the energy demand results align reasonably well with values found in literature. This suggests that the energy demand results are representative of the basic functionalities of the carbon capture technologies and can be compared to others.

Chapter 5.

Conclusions

This work provide an indication on the suitability of the AMP/DMSO system for the Örtofta CHP plant. Because of the novelty of the system and assumptions made in the method, various uncertainties leads to the need for validation of the estimations.

The amount of CO_2 that can be captured from the plant is not a limiting factor. As can be shown by the results, the plant is able to capture 90 % of the CO_2 from the flue gas stream.

The energy requirements of the AMP/DMSO system is comparable to other amine absorption technologies for carbon capture. This system is, however, the only one of the compared systems that can utilize the heat from the DH streams directly. Due to the heat integration possibility this implies, this process is more energy efficient than other aqueous absorption system.

More space is needed for the AMP/DMSO process than comparable systems due to the addition of the phase separator. In this work, a thickener has been used as phase separator. The diameter of this unit is estimated to 120 m, which is substantial. In the sensitivity analysis, it was shown that a much smaller thickener could be obtained. If space requirement is an issue, alternative equipment needs to be considered.

The CAPEX estimation of comparable units between the AMP/DMSO and MEA system shows that the AMP/DMSO process is more expensive than the MEA process when applied to this configuration. The reason is mainly due to the large thickener unit. Because the desorption is estimated to be cheaper for the AMP/DMSO process, it should be considered promising. Sensitivity analysis have shown that the cost of the phase separator could be substantially lower than estimated.

Ultimately, the study concludes that the AMP/DMSO is a very promising system for CCS at the Örtofta CHP plant, mainly due to the energy requirements and integration possibility with the DH streams. Further research, analysis and optimization is required in order to assess the economic feasibility of the plant.

Chapter 6.

Future Work

AMP/DMSO is a novel system for carbon capture. Many uncertainties regarding the system makes process design and rigorous modelling hard to do. Further research are needed on the system, including reaction kinetics, desorption heat and more particle data.

Partial capture is an alternative route that could be considered. In this work, 90 % of the CO_2 is separated in the CCS plant. The reason for this figure is that most other work on this subject use this, making it easy to compare technologies. A suggestion is to look at the available heat and use that as framework in order to estimate how much CO_2 that can be captured.

It is important to consider not only the carbon capture process but also the potential uses for the captured CO_2. A parallel master's thesis investigated the utilization of captured CO2 (CCU) at the Örtofta CHP facility, which initiated further research on this topic.

Further consideration needs to be made towards the phase separator. This unit is of high importance due to its direct effect on the energy demand of the process. A thickener, that has been used in this work, is a very simple unit which has the advantage of being manageable and cheap. Other phase separating units needs to be considered because of the slow settling of particles. Two suggested units are: hydrocyclone and lamella sedimentation tank.

BECCS is, to say the least, a subject of current high focus of discussion. Because of the progress made in this field it should be of interest of companies and stakeholders to be apart of this national and global transition. Kraftringen are now planning an expansion of Örtofta CHP, which makes CCS less prioritized at this site for now. However, given the relationship between Kraftringen and the Departments of Chemical Engineering and Energy Sciences at LTH, it should be feasible to continue to research in this field. A recommendation of the author is to initiate a cooperative planning of a AMP/DMSO pilot plant for further research.

Bibliography

[1] I. P. on Climate Change, "Global warming of 1.5°c", IPCC, Special Report SR1.5, 2018. [Online]. Available: https://www.ipcc.ch/sr15/.

[2] L. Clarke, K. Jiang, K. Akimoto *et al.*, "Assessing transformation pathways", 2014.

[3] G. P. Peters, R. M. Andrew, J. G. Canadell *et al.*, "Key indicators to track current progress and future ambition of the paris agreement", *Nature Climate Change*, vol. 7, no. 2, pp. 118–122, 2017.

[4] S. Fuss, J. G. Canadell, G. P. Peters *et al.*, "Negative emissions—part 2: Costs, potentials and side effects", *Environmental Research Letters*, vol. 13, no. 6, p. 063 002, 2018. DOI: 10.1088/1748-9326/aabf9b.

[5] P. Smith, S. J. Davis, F. Creutzig *et al.*, "Biological mitigation of greenhouse gases: A briefing note for policymakers", *Carbon Management*, vol. 7, no. 1, pp. 49–61, 2016. DOI: 10.1080/17583004.2016.1150797.

[6] "Kraftringen ab - örtofta", Kraftringen AB. (2023), [Online]. Available: https://www.kraftringen.se/om-kraftringen/om-oss/vara-anlaggningar/ortoftaverket/.

[7] B. Everett and O. University, *Energy Systems and Sustainability: Power for a Sustainable Future* (#X98;Theœ open university). OUP Oxford, 2012, ISBN: 9780199593743. [Online]. Available: https://books.google.se/books?id=ZClauQAACAAJ.

[8] "Örtofta kraftvärmeverk ska leverera industriånga till nordic sugar", Nordiska Projekt AB. (2021), [Online]. Available: https://www.nordiskaprojekt.se/2021/09/28/ortofta-kraftvarmeverk-ska-leverera-industrianga-till-nordic-sugar/.

[9] Kraftringen, *Örtofta*, https://www.kraftringen.se/foretag/vara-produktionsanlaggningar/kraftvarmeortofta/, Accessed: April 20, 2023, 2021.

[10] J. Wilcox, *Carbon Capture. [Elektronisk resurs].* Springer New York, 2012, ISBN: 9781461422143. [Online]. Available: http://ludwig.lub.lu.se/login?url=https://search.ebscohost.com/login.aspx?direct=true&AuthType=ip,uid&db=cat07147a&AN=lub.6009245&site=eds-live&scope=site.

[11] L. M. Romeo, I. Bolea and J. M. Escosa, "Integration of power plant and amine scrubbing to reduce co2 capture costs", *Applied Thermal Engineering*, vol. 28, no. 8, pp. 1039–1046, 2008. DOI: 10.1016/j.applthermaleng.2007.06.036.

[12] M. Sanku, "Methodologies for non-aqueous systems and precipitating systems as carbon capture technologies : A case-study of amp-nmp", *Methodologies for Non-aqueous Systems and Precipitating Systems as Carbon Capture Technologies : A case-study of AMP-NMP*, 2020. [Online]. Available: https://lup.lub.lu.se/search/publication/67af341b-b0cc-4668-80c9-71f6cbef9407.

[13] H. Karlsson, *Precipitating Amine Absorption Systems for Carbon Capture.* Department of Chemical Engineering, Faculty of Engineering, Lund University, 2021, pp. 5–17, ISBN: 9789174228397. [Online]. Available: http://ludwig.lub.lu.se/login?url=https://search.ebscohost.com/login.aspx?direct=true&db=cat07147a&AN=lub.6920379&site=eds-live&scope=site, (accessed: 4.1.2022).

[14] H. K. Karlsson, M. G. Sanku and H. Svensson, "Absorption of carbon dioxide in mixtures of n-methyl-2-pyrrolidone and 2-amino-2-methyl-1-propanol", *International Journal of Greenhouse Gas Control*, vol. 95, p. 102 952, 2020, ISSN: 1750-5836. DOI: https://doi.org/10.1016/j.ijggc.2019.102952. [Online]. Available: https://www.sciencedirect.com/science/article/pii/S1750583619304499.

[15] H. e. Karlsson, "Precipitating non-aqueous amine systems for absorption of carbon dioxide using 2-amino-2-methyl-1-propanol.", *International Journal of Greenhouse Gas Control*, vol. 88, pp. 460–468, 2019, ISSN: 17505836. [Online]. Available: http://ludwig.lub.lu.se/login?url=https://search.ebscohost.com/login.aspx?direct=true&AuthType=ip,uid&db=edselc&AN=edselc.2-52.0-85068599186&site=eds-live&scope=site.

[16] H. K. Karlsson, H. Makhool, M. Karlsson and H. Svensson, "Chemical absorption of carbon dioxide in non-aqueous systems using the amine 2-amino-2-methyl-1-propanol in dimethyl sulfoxide and n-methyl-2-pyrrolidone.", *Separation and Purification Technology*, vol. 256, 2021, ISSN: 1383-5866. [Online]. Available: http://ludwig.lub.lu.se/login?url=https://search.ebscohost.com/login.aspx?direct=true&AuthType=ip,uid&db=edsswe&AN=edsswe.oai.lup.lub.lu.se.e237d646.3ae8.4a59.8626.e8d5fd3e153a&site=eds-live&scope=site.

[17] H. Karlsson and H. Svensson, "Rate of absorption for co2 absorption systems using a wetted wall column.", *Energy Procedia*, vol. 114, pp. 2009 –2023, 2017, ISSN: 1876-6102. [Online]. Available: http://ludwig.lub.lu.se/login?url=https://search.ebscohost.com/login.aspx?direct=true&AuthType=ip,uid&db=edsswe&AN=edsswe.oai.lup.lub.lu.se.7637fd8e.f970.4c8a.abb2.ca354f45c9f8&site=eds-live&scope=site.

[18] *Risk management of n-methylpyrrolidone (nmp) - u.s. environmental protection agency*, https://www.epa.gov/assessing-and-managing-chemicals-under-tsca/risk-management-n-methylpyrrolidone-nmp, Accessed on: 2023-04-12.

[19] Captimise, "Capture ready chp design", Unpublished Internal document, 2023.

[20] J. G. Thompson, X. Gao, S. Toma *et al.*, "Decomposition of n-nitrosamines formed in co2 capture systems through electrochemically-mediated reduction on carbon xerogel electrode", *International Journal of Greenhouse Gas Control*, vol. 83, pp. 83–90, 2019, ISSN: 1750-5836. DOI: https://doi.org/10.1016/j.ijggc.2019.02.003. [Online]. Available: https://www.sciencedirect.com/science/article/pii/S1750583618306911.

[21] S. Toma, A. Omosebi, X. Gao *et al.*, "Targeted electrochemical reduction of carcinogenic n-nitrosamines from emission control systems within co2 capture plants", *Chemosphere*, vol. 333, p. 138 915, 2023, ISSN: 0045-6535. DOI: https://doi.org/10.1016/j.chemosphere.2023.138915. [Online]. Available: https://www.sciencedirect.com/science/article/pii/S0045653523011827.

[22] M. Alveteg, *Handbook*. Department of Chemical Engineering, Faculty of Engineering, Lund University, 2017.

[23] R. Smith, "Chemical process: Design and integration", in Wiley, 2005, ISBN: 9780470011911. [Online]. Available: https://books.google.se/books?id=cdyiWR0d1o8C.

[24] Nilsson, Frida, *Evaluation of Excess Heat Driven Carbon Capture Integrated at a Swedish Pulp Mill*, eng, Student Paper, 2023.

[25] J. D. Seader, E. J. Healey and D. K. Roper, "Separation process principles", in 3rd. John Wiley & Sons, 2010.

[26] G. Ulrich, *Chemical Engineering Process Design and Economics: A Practical Guide*. Process Publishing, 2004, ISBN: 9780970876812. [Online]. Available: https://books.google.se/books?id=27kvAAAACAAJ.

[27] H. Svensson and H. Karlsson, "Absorption with chemical reaction", Unpublished Course Document, 2019.

[28] B. Nilsson and N. Andersson, *Applied Transport Phenomenon*. Lund University, Chemical Engineering, 2020.

[29] R. Smith, "Chemical process: Design and integration", in Wiley, 2005, ch. Separation of Hetrogenous Mixtures, ISBN: 9780470011911. [Online]. Available: https://books.google.se/books?id=cdyiWR0d1o8C.

[30] Robertsson, Erik, *Experimental assessment of properties for a non-aqueous and precipitating alkanolamine absorption system*, eng, Student Paper, 2022.

[31] J. D. Seader, E. J. Healey and D. K. Roper, in ch. Mechanical Phase Separations.

[32] L. Liu, M. A. Perez and J. B. Whitman, "Evaluation of lamella settlers for treating suspended sediment", *Water*, vol. 12, no. 10, 2020, ISSN: 2073-4441. DOI: 10.3390/w12102705. [Online]. Available: https://www.mdpi.com/2073-4441/12/10/2705.

[33] E. s.r.o., *Lamella sedimentation tanks and clarifiers*, Online, Accessed 2023. [Online]. Available: https://envites.cz/en/lamella-sedimentation-tanks-and-clarifiers.

[34] E. Gregersen, "Stokes's law", *Encyclopedia Britannica*, 2021. [Online]. Available: https://www.britannica.com/science/Stokess-law.

[35] "Chapter 8 - sedimentation", in *Coulson and Richardson's Chemical Engineering (Sixth Edition)*, R. Chhabra and M. G. Basavaraj, Eds., Sixth Edition, Butterworth-Heinemann, 2019, pp. 387–447, ISBN: 978-0-08-101098-3. DOI: https://doi.org/10.1016/B978-0-08-101098-3.00009-3. [Online]. Available: https://www.sciencedirect.com/science/article/pii/B9780081010983000093.

[36] R. Billet, "Evaporation", in *Ullmann's Encyclopedia of Industrial Chemistry*. John Wiley Sons, Ltd, 2000, ISBN: 9783527306732. DOI: https://doi.org/10.1002/14356007.b03_03. eprint: https://onlinelibrary.wiley.com/doi/pdf/10.1002/14356007.b03_03. [Online]. Available: https://onlinelibrary.wiley.com/doi/abs/10.1002/14356007.b03_03.

[37] M. Alveteg, *Introduction to transport phenomena and separation processes*. Department of Chemical Engineering, Faculty of Engineering, Lund University, 2021.

[38] M. Biermann, F. Normann, F. Johnsson and R. Skagestad, "Partial carbon capture by absorption cycle for reduced specific capture cost", *Industrial & Engineering Chemistry Research*, vol. 57, no. 45, pp. 15 411–15 422, 2018. DOI: 10.1021/acs.iecr.8b02074. eprint: https://doi.org/10.1021/acs.iecr.8b02074. [Online]. Available: https://doi.org/10.1021/acs.iecr.8b02074.

[39] M. Biermann, *Partial CO 2 Capture to Facilitate Cost-Efficient Deployment of Carbon Capture and Storage in Process Industries-Deliberations on Process Design, Heat Integration, and Carbon Allocation*. Chalmers Tekniska Hogskola (Sweden), 2022.

[40] J. N. Knudsen and P. Vilhelmsen, "First year operation experience with a 1 t/h co2 absorption pilot plant at esbjerg coal-fired power plant", in *European Congress of Chemical Engineering*, 2007, pp. 16–20.

[41] A. Bahadori, "Chapter 10 - natural gas sweetening", in *Natural Gas Processing*, A. Bahadori, Ed., Boston: Gulf Professional Publishing, 2014, pp. 483–518, ISBN: 978-0-08-099971-5. DOI: https://doi.org/10.1016/B978-0-08-099971-5.00010-6. [Online]. Available: https://www.sciencedirect.com/science/article/pii/B9780080999715000106.

[42] Skärvad, Per Hugo, *Företagsekonomi 100*, swe. Liber, 2016, ISBN: 978-91-47-08795-2.

[43] M. Bui, C. S. Adjiman, A. Bardow *et al.*, "Carbon capture and storage (ccs): The way forward", *Energy & Environmental Science*, vol. 11, no. 5, pp. 1062–1176, 2018. DOI: 10.1039/c7ee02342a.

[44] R. Newburgh and H. Leff, "The mayer-joule principle: The foundation of the first law of thermodynamics", *The Physics Teacher*, vol. 49, pp. 484–487, Nov. 2011. DOI: 10.1119/1.3651729.

[45] D. J. Heldebrant, P. K. Koech, V.-A. Glezakou, R. Rousseau, D. Malhotra and D. C. Cantu, "Water-lean solvents for post-combustion co2 capture: Fundamentals, uncertainties, opportunities, and outlook", *Chemical Reviews*, vol. 117, no. 14, pp. 9594–9624, 2017, PMID: 28627179. DOI: 10.1021/acs.chemrev.6b00768. eprint: https://doi.org/10.1021/acs.chemrev.6b00768. [Online]. Available: https://doi.org/10.1021/acs.chemrev.6b00768.

[46] H. L. Clever and E. F. J. Westrum, "Dimethyl sulfoxide and dimethyl sulfone. heat capacities, enthalpies of fusion, and thermodynamic properties", *The Journal of Physical Chemistry*, vol. 74, no. 6, pp. 1309–1317, 1970. DOI: 10.1021/j100701a027. eprint: https://doi.org/10.1021/j100701a027. [Online]. Available: https://doi.org/10.1021/j100701a027.

Appendix A.

Mass Balance and Energy Balance Calculations

The mass balance and energy balance calculations for each stream (F#) and heat exchanger (HEX#) in Figure A.1 is presented in Table A.1.

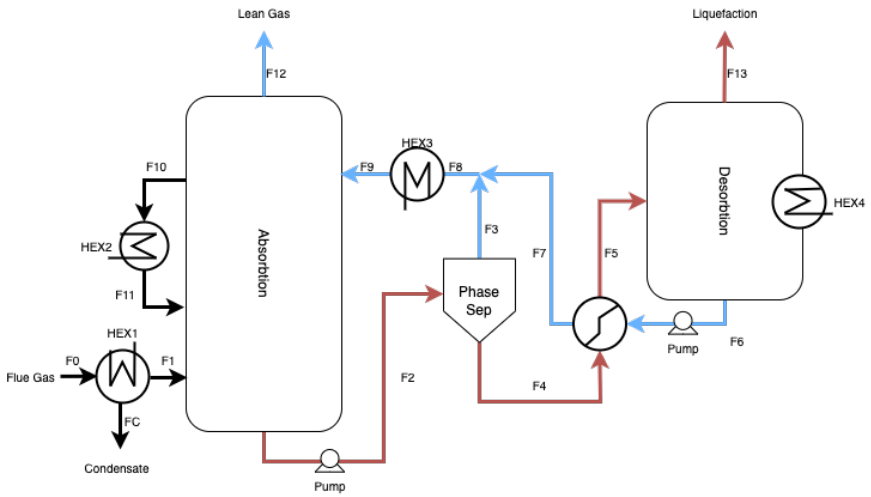

Figure A.1.: Flowsheet of AMPDMSO system used for the mass and energy balance calculations.

Table A.1.: Mass balance for the streams together with the corresponding temperatures and specific heat capacities of the streams. The streams are illustrated in Figure A.1 above.

Stream	Component	Mass Flow (kg/s)	Molar Flow (kmole/s)	x_i / y_i	T (C)	Specific Heat Capacity (J/molK)
F0	air	48,25	1,67	0,77	45	35
	CO2	12,38	0,28	0,13		
	H2O	3,90	0,22	0,1		

	Amp	0,00	0,00	0		
	Dmso	0,00	0,00	0		
	tot	64,52	2,16	1		
FC	air	0,00	0,00	0,00	25	75
	CO2	0,00	0,00	0,00		
	H2O	3,90	0,22	1,00		
	Amp	0,00	0,00	0,00		
	Dmso	0,00	0,00	0,00		
	tot	3,90	0,22	1,00		
F1	air	48,25	1,67	0,84	25	35
	CO2	12,38	0,28	0,14		
	H2o	0,00	0,04	0,02		
	Amp	0,00	0,00	0,00		
	Dmso	0,00	0,00	0,00		
	tot	60,63	1,99	1,00		
F2	air	0,00	0,00	0,00	50	174
	CO2	14,85	0,34	0,08		
	H2O	0,00	0,00	0,00		
	Amp	82,39	1,05	0,25		
	Dmso	247,16	2,77	0,67		
	tot	344,39	4,16	1,00		
F3	air	0,00	0,00	0,00	50	153
	CO2	0,00	0,00	0,00		
	H2O	0,00	0,00	0,00		
	Amp	0,00	0,00	0,00		
	Dmso	222,44	2,50	1,00		
	tot	222,44	2,50	1,00		
F4	air	0,00	0,00	0,00	50	214
	CO2	14,85	0,34	0,20		
	H2O	0,00	0,00	0,00		
	Amp	82,39	1,05	0,63		
	Dmso	24,72	0,28	0,17		
	tot	121,95	1,67	1,00		
F5	air	0,00	0,00	0,00	74	213,64
	CO2	14,85	0,34	0,20		
	H2O	0,00	0,00	0,00		
	Amp	82,39	1,05	0,63		
	Dmso	24,72	0,28	0,17		
	tot	121,95	1,67	1,00		
F6	air	0,00	0,00	0,00	88	214

	CO2	3,71	0,08	0,06		
	H2O	0,00	0,00	0,00		
	Amp	82,39	1,05	0,74		
	Dmso	24,72	0,28	0,20		
	tot	110,81	1,42	1,00		
F7	air	0,00	0,00	0,00	60	214
	CO2	3,71	0,08	0,06		
	H2O	0,00	0,00	0,00		
	Amp	82,39	1,05	0,74		
	Dmso	24,72	0,28	0,20		
	tot	110,81	1,42	1,00		
F8	air	0	0	0,00	54	174
	CO2	3,71	0,08	0,02		
	H2O	0	0	0,00		
	Amp	82,39	1,05	0,27		
	Dmso	247,16	2,77	0,71		
	tot	333,26	3,91	1,00		
F9	air	0,00	0,00	0,00	40	174
	CO2	3,71	0,08	0,02		
	H2O	0,00	0,00	0,00		
	Amp	82,39	1,05	0,27		
	Dmso	247,16	2,77	0,71		
	tot	333,26	3,91	1,00		
F10	air	0,00	0,00	0,00	80	174
	CO2	14,85	0,37	0,09		
	H2O	0,00	0,00	0,00		
	Amp	82,39	1,05	0,25		
	Dmso	247,16	2,77	0,66		
	tot	344,39	4,19	1,00		
F11	air	0,00	0,00	0,00	50	174
	CO2	14,85	0,37	1,00		
	H2O	0,00	0,00	0,00		
	Amp	82,39	0,00	0,00		
	Dmso	247,16	0,00	0,00		
	tot	344,39	0,37	1,00		
F12	air	48,25	1,67	0,96	50	
	CO2	1,24	0,03	0,02		
	H2O	0,00	0,04	0,02		
	Amp	0,00	0,00	0,00		
	Dmso	0,00	0,00	0,00		

	tot	49,49	1,73	1,00		
F13	air	0,00	0,00	0,00	88	40
	CO2	11,14	0,25	1,00		
	H2O	0,00	0,00	0,00		
	Amp	0,00	0,00	0,00		
	Dmso	0,00	0,00	0,00		
		0	0,25	1,00		

Appendix B.

Design Parameters

B.1. Absorption Column Height

$$z = \frac{1}{\left(\frac{1}{N_z^G}\right) K_G P_T a_i} ln\left(\frac{y_2}{y_1}\right) \tag{B.1}$$

Table B.1.: Design parameters for the absorption column.

N_z^G (mol/m^2/s)	$K_G \cdot 10^6$ (mol/m^2/s/kPa)	P_T (kPa)	a_i (m^2/m^3)
25	1	101	250

B.2. Thickener

$$A = F_s \left(\frac{\left(\frac{F_l}{F_s}\right) - \left(\frac{0.1F_l}{F_s}\right)}{v_T \rho} \right) \tag{B.2}$$

Table B.2.: Design parameters for the thickener.

F_l (kg/s)	F_s (kg/s)	$v_T \cdot 10^6$ (m/s)	ρ (kg/m^3)
300	45	22	1100

B.3. Evaporator

$$A_h = \frac{Q_{tot}}{(k \cdot \Delta T_{log})} \tag{B.3}$$

Table B.3.: Design parameters for the evaporation column.

Q_{tot} (MW)	k (W/m2/K)	ΔT_{log} (K)
34	1000	14